

Derivatives of maximum-entropy basis functions on the boundary: Theory and computations

F. Greco¹ and N. Sukumar^{2,*}

¹ *Department of Mechanical Engineering, University of Calabria, 87036 Rende (CS), Italy*

² *Department of Civil and Environmental Engineering, University of California, Davis, CA 95616, USA*

SUMMARY

In this paper, we obtain explicit expressions to evaluate the derivatives of maximum-entropy (max-ent) basis function on the boundary of a convex domain. In the max-ent formulation, the basis functions are obtained by maximizing a concave functional subjected to linear constraints (reproducing conditions). In doing so, it is found that the Lagrange multipliers blow up when $\mathbf{x} \in \partial\Omega$, and the expressions for the derivatives of the max-ent basis functions in Ω are of an indeterminate form for points on $\partial\Omega$. We appeal to l'Hôpital's rule to derive expressions to determine the derivatives of the basis functions. We consider the Shannon entropy functional as well as the relative entropy functional with different choices of the *prior* weight function. The first-order derivatives of all basis functions are bounded. In contrast, on an irregular grid with a certain nodal spacing, some of the second-derivatives of the basis functions are unbounded on the boundary. Necessary and sufficient conditions on the *priors* to obtain bounded Lagrange multipliers are established. Optimal convergence rates for fourth-order problems

*Correspondence to: N. Sukumar, Department of Civil and Environmental Engineering, University of California, One Shields Avenue, Davis, CA 95616, USA. E-mail: nsukumar@ucdavis.edu

are demonstrated for a Galerkin approach with a quadratically complete partition-of-unity enriched max-ent approximation. Copyright © 2013 John Wiley & Sons, Ltd.

KEY WORDS: maximum-entropy principle, relative entropy, convex approximation, plate bending, meshfree method, l'Hôpital's rule

1. INTRODUCTION

Within the family of meshfree approximation methods [1, 2], a recent advance in computational mechanics has been the development and application of maximum-entropy (max-ent) based approximation schemes [3–6]. These approximations are linked to elements from information theory [7], convex analysis [8], and convex optimization [9]. Initially, these convex approximants were introduced by Sukumar [3] for constructing polygonal interpolants and by Arroyo and Ortiz [4] for use in meshfree methods. Since then, many new developments and applications of max-ent basis functions have emerged: unifying formulation using relative entropy and an extension to higher-order schemes with signed basis functions [10], quadratically complete convex approximations [11–13], epi-convergence to establish continuity of max-ent basis functions [14] and convergence analysis of max-ent approximation schemes [15, 16], constructing barycentric coordinates on arbitrary polytopes [17], fluid and plastic flow using optimal transportation theory [18], compressible and nearly incompressible elasticity [19–22], variational adaptivity for finite-deformation elasticity [23], thin-shell analysis [24, 25], modeling Mindlin-Reissner shear-deformable plates [26], nonlinear structural analyses [27, 28], convection-diffusion problems [29–31], phase-field model of biomembranes [32], curvature and bending rigidity of membrane networks [33, 34], and Kohn-Sham density functional

calculations [35].

Consider a set of distinct nodes in \mathbb{R}^d that are located at \mathbf{x}_a ($a = 1, 2, \dots, n$), with $\Omega = \text{con}(\mathbf{x}_1, \dots, \mathbf{x}_n) \subset \mathbb{R}^d$ denoting the convex hull of the nodal set. For a real-valued function $u(\mathbf{x}) : \Omega \rightarrow \mathbb{R}$, the numerical approximation for $u(\mathbf{x})$ is:

$$u^h(\mathbf{x}) = \sum_{a=1}^n \phi_a(\mathbf{x}) u_a, \quad (1)$$

where $\phi_a(\mathbf{x})$ is the basis function associated with node a , and u_a are coefficients.

In the maximum-entropy approach [36, 37], an entropy functional (Shannon entropy [7] or negative of the relative entropy [38, 39] that depends on a discrete probability measure $\{p_a\}_{a=1}^n$) is maximized, subject to linear constraints on p_a . On noting the correspondence between basis functions $\{\phi_a\}_{a=1}^n$ and discrete probability measures $\{p_a\}_{a=1}^n$, the max-ent formalism is applied to construct basis functions [3, 4, 10]. To this end, we consider the maximization of the negative of the relative entropy, subject to linear reproducing conditions on $\phi_a(\mathbf{x})$ — $u^h(\mathbf{x})$ in (1) should exactly reproduce affine functions. In doing so, the expressions for the basis functions and their derivatives are readily derived, which are found to depend on the solution of the Lagrange multipliers $\boldsymbol{\lambda}(\mathbf{x}) \in \mathbb{R}^d$ (details are provided in Section 2). As noted in References [3] and [4], the Lagrange multipliers blow up for a point $\mathbf{x} \in \partial\Omega$, and hence the expressions derived therein for $\nabla\phi_a$ can not be used to evaluate the derivatives of the basis functions on the boundary. In this paper, a solution for this problem is provided. We apply l'Hôpital's rule to obtain explicit expressions for the derivatives of the basis functions on the boundary, which is guided by theoretical analysis and supportive numerical experiments. Furthermore, on choosing appropriate *prior* weight functions [37, 10], we present a means to obtain bounded Lagrange multipliers on the boundary, which leads to bounded first- and higher-order derivatives of max-ent basis functions on $\partial\Omega$. Optimal convergence rates for Euler-Bernoulli beam problems

and for plate bending problems are demonstrated for a Galerkin approach with a quadratically complete partition-of-unity enriched max-ent approximation.

2. MAXIMUM-ENTROPY BASIS FUNCTIONS

We use the relative entropy functional [38] to construct max-ent basis functions. The variational formulation for maximum-entropy approximants is: find $\boldsymbol{\phi}(\mathbf{x}) : \Omega \rightarrow \mathbb{R}_+^n$ as the solution of the following constrained (concave) optimization problem [4, 10]:

$$\max_{\boldsymbol{\phi} \in \mathbb{R}_+^n} - \sum_{a=1}^n \phi_a(\mathbf{x}) \ln \left(\frac{\phi_a(\mathbf{x})}{w_a(\mathbf{x})} \right), \quad (2a)$$

subject to the linear reproducing conditions:

$$\sum_{a=1}^n \phi_a(\mathbf{x}) = 1, \quad (2b)$$

$$\sum_{a=1}^n \phi_a(\mathbf{x})(\mathbf{x}_a - \mathbf{x}) = \mathbf{0}, \quad (2c)$$

where \mathbb{R}_+^n is the non-negative orthant, $w_a(\mathbf{x}) : \Omega \rightarrow \mathbb{R}_+$ is a non-negative weight function (*prior estimate* to ϕ_a), and the linear constraints form an underdetermined system. On using the method of Lagrange multipliers, the solution of the variational problem is [10]:

$$\phi_a(\mathbf{x}) = \frac{Z_a(\mathbf{x}; \boldsymbol{\lambda})}{Z(\mathbf{x}; \boldsymbol{\lambda})}, \quad Z_a(\mathbf{x}; \boldsymbol{\lambda}) = w_a(\mathbf{x}) \exp(-\boldsymbol{\lambda} \cdot \tilde{\mathbf{x}}_a) \quad (3)$$

where $\tilde{\mathbf{x}}_a = \mathbf{x}_a - \mathbf{x}$ ($\mathbf{x}, \mathbf{x}_a \in \mathbb{R}^d$) are shifted nodal coordinates, $\boldsymbol{\lambda}(\mathbf{x}) \in \mathbb{R}^d$ are the d Lagrange multipliers associated with the constraints in (2c), and $Z(\mathbf{x}; \boldsymbol{\lambda}) = \sum_b Z_b(\mathbf{x}; \boldsymbol{\lambda})$ is known as the *partition function* in statistical mechanics. On considering the dual formulation, the solution for the Lagrange multipliers can be written as [9]

$$\boldsymbol{\lambda}^* = \operatorname{argmin} F(\boldsymbol{\lambda}), \quad F(\boldsymbol{\lambda}) := \ln Z(\boldsymbol{\lambda}), \quad (4)$$

where $\boldsymbol{\lambda}^*$ is the optimal solution that is desired. Since F is strictly convex in the interior of Ω , a convex optimization algorithm such as Newton's method is used to determine $\boldsymbol{\lambda}^*$.

Let $\phi_a^*(\mathbf{x})$ be the max-ent basis function that corresponds to the converged $\boldsymbol{\lambda}^*(\mathbf{x})$, and $\nabla\phi_a^*(\mathbf{x})$ and $\nabla\nabla\phi_a^*(\mathbf{x})$ be the gradient and Hessian of $\phi_a^*(\mathbf{x})$, respectively. We obtain $\phi_a^*(\mathbf{x})$ from (3):

$$\phi_a^*(\mathbf{x}) = \frac{Z_a(\mathbf{x}; \boldsymbol{\lambda}^*)}{Z(\mathbf{x}; \boldsymbol{\lambda}^*)}, \quad Z_a(\mathbf{x}; \boldsymbol{\lambda}^*) = w_a(\mathbf{x}) \exp(-\boldsymbol{\lambda}^* \cdot \tilde{\mathbf{x}}_a). \quad (5)$$

The gradient of $\phi_a^*(\mathbf{x})$ for the Gaussian prior (*local* max-ent) is presented in Reference [4], and that for an arbitrary prior weight function appears in References [40, 27]. The latter can be written in the following form:

$$\nabla\phi_a^* = \phi_a^* \left\{ \tilde{\mathbf{x}}_a \cdot [(\mathbf{H}^*)^{-1} - (\mathbf{H}^*)^{-1} \cdot \mathbf{A}^*] - \sum_{b=1}^n \frac{\nabla w_b \exp(-\boldsymbol{\lambda}^* \cdot \tilde{\mathbf{x}}_b)}{Z} \right\} + \frac{\nabla w_a \exp(-\boldsymbol{\lambda}^* \cdot \tilde{\mathbf{x}}_a)}{Z} \quad (6a)$$

where

$$\mathbf{H}^* = \sum_{b=1}^n \phi_b^* \tilde{\mathbf{x}}_b \otimes \tilde{\mathbf{x}}_b, \quad \mathbf{A}^* = \sum_{b=1}^n \tilde{\mathbf{x}}_b \otimes \frac{\nabla w_b \exp(-\boldsymbol{\lambda}^* \cdot \tilde{\mathbf{x}}_b)}{Z} \quad (6b)$$

The derivation and expression for the Hessian of $\phi_a^*(\mathbf{x})$ are presented in References [40, 13, 33].

3. ONE-DIMENSIONAL ANALYSIS

Consider a one-dimensional domain Ω that is discretized by a set of nodes with coordinates $\{x_a\}_{a=1}^n$, where $x_1 < x_2 < \dots < x_n$. We seek to evaluate the derivatives of the basis functions $\phi_1(x), \phi_2(x), \dots, \phi_n(x)$ when $x = x_1$ or $x = x_n$.

3.1. On the behavior of λ on the boundary of the domain

The difficulties that arise in the calculation of the derivatives of the basis functions on the boundary of the domain are a consequence of the divergence of the Lagrange multipliers, which is assessed in the following proposition:

Proposition 3.1. *Given prior weight functions $\{w_1(x), w_2(x) \dots w_n(x)\}$ such that $\exists a > 1 : w_a(x_1) \neq 0$, then $\lim_{x \rightarrow x_1} \lambda(x) = +\infty$, and if $\exists a < n : w_a(x_n) \neq 0$, then $\lim_{x \rightarrow x_n} \lambda(x) = -\infty$.*

Proof. First of all we remark that in every maximum entropy approximation, $w_a(x) \geq 0$ for all a and $w_1(x_1) \neq 0$, $w_n(x_n) \neq 0$. These conditions are necessary to meet the convexity condition ($\phi_a(x) \geq 0$ for all a) and the Kronecker-delta property on the boundary, namely $\phi_a(x_1) = \delta_{a1}$ and $\phi_a(x_n) = \delta_{an}$. On substituting $\phi_a(x)$ from (3) in (2c), we have

$$\sum_{a=1}^n w_a(x)(x_a - x)e^{-\lambda(x)(x_a - x)} = 0 \quad (7)$$

When $x \rightarrow x_1$, the above equation becomes

$$\sum_{\substack{a \\ w_a(x_1) \neq 0}}^n w_a(x_1)(x_a - x_1)e^{-\lambda(x_1)(x_a - x_1)} = 0$$

Since $w_a(x_1) > 0$ and $x_a - x_1 > 0$ for all a , the equality in the above equation is met if and only if each term is identically equal to zero. Hence, $e^{-\lambda(x_1)(x_a - x_1)} \rightarrow 0$, which implies that $\lambda(x_1) \rightarrow +\infty$. Following a similar approach for the case $x \rightarrow x_n$, it is readily shown that if $\exists a < n : w_a(x_n) \neq 0$, then $\lim_{x \rightarrow x_n} \lambda(x_n) = -\infty$. \square

3.2. First derivatives of global max-ent

In the global max-ent approximant, the prior weight function $w_a(x) = 1$ for all a . According to Proposition 3.1, since the Lagrange multiplier $\lambda(x) \rightarrow +\infty$ when $x \rightarrow x_1$ and $\lambda(x) \rightarrow -\infty$

when $x \rightarrow x_n$, the derivatives of $\phi_a(x)$ can not be computed using the expression given in (6). We point out that when λ blows up on the boundary, the basis functions too can not be computed from (3). However, the max-ent basis functions in \mathbb{R}^d satisfy a *weak* Kronecker-delta property on the boundary with interior basis functions (facet-reducing property) vanishing on the boundary. This permits the direct evaluation of the basis functions on a facet of reduced dimension. At the boundary $x = x_1$ in one dimension, we obtain: $\phi_1(x_1) = 1, \phi_a(x_1) = 0$ for all $a > 1$. Since the expressions for $\phi'_a(x_1)$ and $\phi'_a(x_n)$ are of an indeterminate form, we define the derivatives on the boundary x_1 as the following limit with $x \rightarrow x_1$ from within the domain:

$$\phi'_a(x_1) \equiv \lim_{x \rightarrow x_1} \phi'_a(x),$$

and we proceed to determine the above limit. Consider

$$\lim_{x \rightarrow x_1} \frac{\phi_a(x)}{\phi_2(x)} \quad \forall a > 2.$$

Since $\phi_a(x_1) = 0$ and $\phi_2(x_1) = 0$, we can apply l'Hôpital's rule to obtain

$$\lim_{x \rightarrow x_1} \frac{\phi_a(x)}{\phi_2(x)} = \lim_{x \rightarrow x_1} \frac{\phi'_a(x)}{\phi'_2(x)} \tag{8}$$

for all $a > 2$. On the other hand, we can determine the above limit using the explicit basis function expressions from (5):

$$\lim_{x \rightarrow x_1} \frac{\phi_a(x)}{\phi_2(x)} = \lim_{x \rightarrow x_1} \frac{Z_a/Z}{Z_2/Z} = \lim_{x \rightarrow x_1} \frac{Z_a}{Z_2} = \lim_{x \rightarrow x_1} \frac{e^{-\lambda(x)x_a}}{e^{-\lambda(x)x_2}} = \lim_{x \rightarrow x_1} e^{-\lambda(x)(x_a - x_2)} \tag{9}$$

Now, since $x_a - x_2 > 0$ and $\lim_{x \rightarrow x_1} \lambda(x) = +\infty$, we have

$$\lim_{x \rightarrow x_1} \frac{\phi_a(x)}{\phi_2(x)} = 0 \quad \forall a > 2$$

and hence (8) can be written as

$$\lim_{x \rightarrow x_1} \frac{\phi'_a(x)}{\phi'_2(x)} = 0 \quad \forall a > 2. \tag{10}$$

Now, we show that $\lim_{x \rightarrow x_1} \phi'_2(x)$ is non-zero. On taking the derivative of the linear reproducing conditions given in Section 2, we obtain

$$\sum_{a=1}^n \phi'_a(x) = 0 \quad (11a)$$

$$\sum_{a=1}^n \phi'_a(x) x_a = 1 \quad (11b)$$

For (11a) and (11b) to be satisfied, it is evident that at least two basis function derivatives must be non-zero, and therefore $\lim_{x \rightarrow x_1} \phi'_2(x) \neq 0$. Hence, (10) yields the result:

$$\phi'_a(x_1) = 0 \quad \forall a > 2. \quad (12)$$

The constraints in (11) can now be written as:

$$\phi'_1(x_1) + \phi'_2(x_1) = 0$$

$$\phi'_1(x_1)x_1 + \phi'_2(x_1)x_2 = 1$$

whose solution is: $\phi'_1(x_1) = -1/(x_2 - x_1)$, $\phi'_2(x_1) = 1/(x_2 - x_1)$. Hence, from the above equations and (12), the complete solution for the derivatives of the basis functions at $x = x_1$ is:

$$\phi'_1(x_1) = -\frac{1}{x_2 - x_1}, \quad \phi'_2(x_1) = \frac{1}{x_2 - x_1}, \quad \phi'_a(x_1) = 0 \quad \forall a > 2 \quad (14)$$

On considering the symmetry of the problem, the derivatives of the basis functions at $x = x_n$ are given by

$$\phi'_n(x_n) = \frac{1}{x_n - x_{n-1}}, \quad \phi'_{n-1}(x_n) = -\frac{1}{x_n - x_{n-1}}, \quad \phi'_a(x_n) = 0 \quad \forall a < n - 1 \quad (15)$$

3.3. Second derivatives of global max-ent

Since $\phi_a(x_1) = \phi'_a(x_1) = 0 \quad \forall a \geq 3$, we have

$$\lim_{x \rightarrow x_1} \frac{\phi_a(x)}{\phi_3(x)} = \lim_{x \rightarrow x_1} \frac{\phi'_a(x)}{\phi'_3(x)} = \lim_{x \rightarrow x_1} \frac{\phi''_a(x)}{\phi''_3(x)} = \lim_{x \rightarrow x_1} e^{-\lambda(x)(x_a - x_3)} = e^{-\lambda(x_1)(x_a - x_3)} = 0 \quad (16)$$

for all $a > 3$, since $\lambda(x_1) = \infty$ and $x_a - x_3 > 0$. Therefore, if we assume that $\phi_3''(x_1)$ is finite, then it follows that $\phi_a''(x) = 0$ for all $a > 3$, and now we only need to compute the second derivatives for the first three nodes. On taking the derivatives of the constraint equations in (11), we have

$$\phi_1''(x) + \phi_2''(x) + \phi_3''(x) = 0 \quad (17a)$$

$$\phi_1''(x)x_1 + \phi_2''(x)x_2 + \phi_3''(x)x_3 = 0 \quad (17b)$$

and hence we have one more unknown than the number of equations. To determine the additional relation, we perform some algebra. To wit, we write

$$\phi_3''(x_1) = \lim_{x \rightarrow x_1} \frac{\phi_3'(x)}{x - x_1} = \lim_{x \rightarrow x_1} \frac{\phi_2'(x) \phi_3'(x)}{\phi_2'(x) x - x_1} = \frac{\phi_2'(x_1)}{\lim_{x \rightarrow x_1} \frac{\phi_2'(x)(x-x_1)}{\phi_3'(x)}} \quad (18)$$

where the first equality follows by l'Hôpital's rule and $\phi_2'(x_1) \neq 0$ is used to arrive at the second equality. Now, let us consider $\lim_{x \rightarrow x_1} \frac{\phi_2'(x)(x-x_1)}{\phi_3'(x)}$. Since this is a 0/0 indeterminate form, we can apply l'Hôpital's rule to obtain

$$\lim_{x \rightarrow x_1} \frac{\phi_2'(x)(x-x_1)}{\phi_3'(x)} = \lim_{x \rightarrow x_1} \frac{\phi_2'(x_1)(x-x_1)}{\phi_3'(x)} + \frac{\phi_2(x)}{\phi_3'(x)}$$

Consider the Taylor series of $\phi_3(x)$ and $\phi_3'(x)$ when $x \rightarrow x_1$, cognizant of the fact that $\phi_3(x_1) = \phi_3'(x_1) = 0$:

$$\phi_3(x) = \frac{1}{2}\phi_3''(x_1)(x-x_1)^2 + O(x-x_1)^3$$

$$\phi_3'(x) = \phi_3''(x_1)(x-x_1) + O(x-x_1)^2$$

Combining the above equations, we can write:

$$2\phi_3(x) = \phi_3'(x)(x-x_1) + O(x-x_1)^3$$

Thus, when $x \rightarrow x_1$, $\phi_3'(x) = \frac{2\phi_3(x)}{x-x_1}$ and hence

$$\lim_{x \rightarrow x_1} \frac{\phi_2'(x)}{\phi_3'(x)} = \lim_{x \rightarrow x_1} \frac{\phi_2'(x)(x-x_1)}{2\phi_3(x)}$$

Therefore,

$$\lim_{x \rightarrow x_1} \frac{\phi_2'(x)(x-x_1)}{\phi_3'(x)} = \lim_{x \rightarrow x_1} \frac{\phi_2(x)(x-x_1)}{\phi_3(x)} - \frac{\phi_2(x)(x-x_1)}{2\phi_3(x)} = \lim_{x \rightarrow x_1} \frac{\phi_2(x)(x-x_1)}{2\phi_3(x)}$$

Now, from the above equation and (18), we have

$$\phi_3''(x_1) = \frac{2\phi_2'(x_1)}{\lim_{x \rightarrow x_1} \frac{\phi_2(x)(x-x_1)}{\phi_3(x)}} \quad (19)$$

For global max-ent, the denominator in the above equation is:

$$\lim_{x \rightarrow x_1} \frac{\phi_2(x)(x-x_1)}{\phi_3(x)} = \lim_{x \rightarrow x_1} \frac{x-x_1}{e^{-\lambda(x_3-x_2)}}$$

Recall that

$$x = \frac{\sum_{a=1}^n x_a e^{-\lambda x_a}}{\sum_{a=1}^n e^{-\lambda x_a}} = \frac{x_1 e^{-\lambda x_1} + x_2 e^{-\lambda x_2} \dots + x_n e^{-\lambda x_n}}{e^{-\lambda x_1} + e^{-\lambda x_2} \dots + e^{-\lambda x_n}}$$

and $\lim_{\lambda \rightarrow \infty} e^{-\lambda x_a} / e^{-\lambda x_b} = 0$ when $x_a > x_b$. Then, the above equation can be written (to leading order) as

$$x = \frac{x_1 e^{-\lambda x_1} + x_2 e^{-\lambda x_2} \dots + x_n e^{-\lambda x_n}}{e^{-\lambda x_1} + e^{-\lambda x_2} \dots + e^{-\lambda x_n}} \sim \frac{x_1 e^{-\lambda x_1} + x_2 e^{-\lambda x_2}}{e^{-\lambda x_1} + e^{-\lambda x_2}}$$

and therefore

$$\begin{aligned} \lim_{x \rightarrow x_1} \frac{\phi_2(x)(x-x_1)}{\phi_3(x)} &= \lim_{x \rightarrow x_1} \frac{x-x_1}{e^{-\lambda(x_3-x_2)}} = \lim_{x \rightarrow x_1} \frac{\frac{x_1 e^{-\lambda x_1} + x_2 e^{-\lambda x_2}}{e^{-\lambda x_1} + e^{-\lambda x_2}} - x_1}{e^{-\lambda(x_3-x_2)}} = \lim_{x \rightarrow x_1} \frac{(x_2-x_1)e^{-\lambda x_2}}{e^{-\lambda(x_3-x_2)}} \\ &= \lim_{x \rightarrow x_1} (x_2-x_1) \frac{e^{-\lambda(x_2-x_1)}}{e^{-\lambda(x_3-x_2)}} = \lim_{x \rightarrow x_1} (x_2-x_1) e^{-\lambda[(x_2-x_1)-(x_3-x_2)]} \end{aligned}$$

Since, according to Proposition 3.1, $\lambda \rightarrow \infty$ we note that the above limit is finite and non-zero if and only if $x_2 = (x_1 + x_3)/2$ ($x_2 - x_1 = x_3 - x_2$), in which case

$$\lim_{x \rightarrow x_1} \frac{\phi_2(x)(x-x_1)}{\phi_3(x)} = x_2 - x_1$$

and from (17) and (19), we find that for this case the second derivatives are finite and non-zero:

$$\phi_1''(x_1) = \phi_3''(x_1) = \frac{2}{(x_2 - x_1)^2}, \quad \phi_2''(x_1) = \frac{-4}{(x_2 - x_1)^2} \quad (20)$$

If $x_2 < (x_1 + x_3)/2$, then $\lim_{x \rightarrow x_1} \frac{x-x_1}{e^{-\lambda(x_3-x_2)}} = \infty$ and therefore

$$\phi_1''(x_1) = \phi_2''(x_1) = \phi_3''(x_1) = 0$$

and if $x_2 > (x_1 + x_3)/2$, then $\lim_{x \rightarrow x_1} \frac{x-x_1}{e^{-\lambda(x_3-x_2)}} = 0$, and this implies that the second derivatives are *unbounded* when $x \rightarrow x_1$:

$$|\phi_1''(x_1)|, |\phi_2''(x_1)|, |\phi_3''(x_1)| \rightarrow \infty$$

Remark Using (20), on a regular grid we have the equality

$$\phi_1''(x_1)x_1^2 + \phi_2''(x_1)x_2^2 + \phi_3''(x_1)x_3^2 = 4$$

On observing that $\phi_1(x_1)x_1^0 = 1$ and $\phi_1'(x_1)x_1 + \phi_2'(x_1)x_2 = 1$, we hypothesize the following relation:

$$\sum_{a=1}^{m+1} \frac{d^m \phi_a(x_1)}{dx^m} x_a^m = (m!)^2 \quad (21)$$

which has been numerically verified for $m > 2$.

3.4. Derivatives of local max-ent

The *local* max-ent scheme of Arroyo and Ortiz [4] is identical to use of a Gaussian prior weight function in (2) [6, 10]. Hence, on using $w_a(x) = e^{-\beta(x)(x-x_a)^2}$ in (9), we obtain

$$\lim_{x \rightarrow x_1} \frac{\phi_a(x)}{\phi_2(x)} = \lim_{x \rightarrow x_1} \frac{e^{-\beta(x_1-x_a)^2}}{e^{-\beta(x_1-x_2)^2}} \lim_{x \rightarrow x_1} e^{-\lambda(x_a-x_2)}$$

Since w_a meets the hypotheses of Proposition 3.1, we have $\lim_{x \rightarrow x_1} \lambda(x) = +\infty$, and therefore

$$\lim_{x \rightarrow x_1} \frac{\phi_a(x)}{\phi_2(x)} = 0$$

This reveals that for the *local* max-ent approximation (as in global max-ent), only $\phi_1(x)$ and $\phi_2(x)$ have a non-zero derivative at $x = x_1$. Proceeding likewise, it is readily shown that the

boundary-behavior of $\phi_a''(x)$ in *local* max-ent is similar to that in global max-ent. We provide the expressions for the second derivatives by deriving the limit in (19):

$$\lim_{x \rightarrow x_1} \frac{\phi_2(x)(x-x_1)}{\phi_3(x)} = \lim_{x \rightarrow x_1} (x-x_1) \frac{w_2 e^{-\lambda x_2}}{w_3 e^{-\lambda x_3}} = \lim_{x \rightarrow x_1} \frac{x-x_1}{e^{-\lambda(x_3-x_2)}} \frac{e^{-\beta(x_1-x_2)^2}}{e^{-\beta(x_1-x_3)^2}}$$

and

$$\begin{aligned} \lim_{x \rightarrow x_1} \frac{x-x_1}{e^{-\lambda(x_3-x_2)}} &= \lim_{x \rightarrow x_1} \frac{\frac{w_1 x_1 e^{-\lambda x_1} + w_2 x_2 e^{-\lambda x_2}}{w_1 e^{-\lambda x_1} + w_2 e^{-\lambda x_2}} - x_1}{e^{-\lambda(x_3-x_2)}} \\ &= \lim_{x \rightarrow x_1} \frac{\frac{w_2(x_2-x_1)e^{-\lambda x_2}}{w_1 e^{-\lambda x_1} + w_2 e^{-\lambda x_2}}}{e^{-\lambda(x_3-x_2)}} = \lim_{x \rightarrow x_1} \frac{w_2}{w_1} (x_2-x_1) \frac{e^{-\lambda(x_2-x_1)}}{e^{-\lambda(x_3-x_2)}} \end{aligned}$$

As in the case of global max-ent, the above limit is finite and non-zero if and only if $x_2 = (x_1 + x_3)/2$. In this case, we have

$$\lim_{x \rightarrow x_1} \frac{\phi_2(x)(x-x_1)}{\phi_3(x)} = \lim_{x \rightarrow x_1} \frac{w_2^2}{w_1 w_3} (x_2-x_1) = \frac{[e^{-\beta(x_1-x_2)^2}]^2}{e^{-\beta(x_1-x_3)^2}} (x_2-x_1) = e^{2\beta(x_2-x_1)^2} (x_2-x_1),$$

where $\beta \equiv \beta(x_1)$ in the above equation, and the second derivatives of the basis functions are:

$$\phi_1''(x_1) = \phi_3''(x_1) = \frac{2e^{-2\beta(x_2-x_1)^2}}{(x_2-x_1)^2}, \quad \phi_2''(x_1) = \frac{-4e^{-2\beta(x_2-x_1)^2}}{(x_2-x_1)^2} \quad (22)$$

The *local* max-ent results when $x_2 < (x_1 + x_3)/2$ or $x_2 > (x_1 + x_3)/2$ mirror those derived for global max-ent in Section 3.3.

3.5. Derivatives of max-ent approximants with a general prior weight function

We now refer to the general case in which a prior weight function $w_a(x)$ is associated to each node, and the expression for the max-ent basis function takes the form [10]:

$$\phi_a(x) = \frac{Z_a(x)}{Z(x)} = \frac{w_a(x)e^{-\lambda(x)x_a}}{\sum_{b=1}^n w_b(x)e^{-\lambda(x)x_b}}$$

and we have

$$\lim_{x \rightarrow x_1} \frac{\phi_a'(x)}{\phi_2'(x)} = \lim_{x \rightarrow x_1} \frac{\phi_a(x)}{\phi_2(x)} = \lim_{x \rightarrow x_1} \frac{w_a(x)e^{-\lambda(x)x_a}}{w_2(x)e^{-\lambda(x)x_2}} = \lim_{x \rightarrow x_1} \frac{w_a(x)}{w_2(x)} \lim_{x \rightarrow x_1} e^{-\lambda(x)(x_a-x_2)} \quad (23)$$

for all $a > 2$. In order to correctly evaluate this limit we have to consider the behavior of the two limits involved in the product. Thus, we have to study the limit of the ratio of the *priors* and $\lim_{x \rightarrow x_1} \lambda(x)$. From Proposition 3.1, we arrive at a necessary condition for λ to be bounded at $x = x_1$ and at $x = x_n$:

$$w_a(x_1) = 0 \quad \forall a > 1, \quad w_a(x_n) = 0 \quad \forall a < n \quad (24)$$

However, this condition is not sufficient by itself. We provide a complete set of conditions via the following proposition:

Proposition 3.2. *Let $I = \{1, 2, \dots, n\}$ denote the nodal index set and*

$$I_O = \{a : w_a(x) = O(x - x_b)\} \quad (25a)$$

$$w_a(x) = o(x - x_b) \quad \forall a \in I \setminus \{b\} - I_O \quad (25b)$$

Then, $\lim_{x \rightarrow x_b} |\lambda(x)| < \infty$ ($b = 1, n$), if and only if I_O is non-empty.

Proof. Consider the constraint equation in (7), which can be rewritten as

$$\frac{\sum_{a \in I \setminus \{b\}} w_a(x)(x_a - x)e^{-\lambda(x)x_a}}{w_b(x)(x - x_b)e^{-\lambda(x)x_b}} = 1$$

where $b = 1$ or $b = n$ since we seek the limit of $\lambda(x)$ as $x \rightarrow x_1$ or $x \rightarrow x_n$. Taking the limit $x \rightarrow x_b$, the above equation becomes

$$\sum_{a \in I \setminus \{b\}} \lim_{x \rightarrow x_b} \left[\frac{w_a(x)}{(x - x_b)} \right] (x_a - x_b)e^{-\lambda(x_b)(x_a - x_b)} = w_b(x_b) \quad (26)$$

If (25) is met with I_O non-empty, then $\lim_{x \rightarrow x_b} \frac{w_a(x)}{(x - x_b)} = C_{ab}$ (finite) if $a \in I_O$ and zero otherwise. Therefore, a bounded $\lambda \equiv \lambda(x_b)$ solves the nonlinear equation

$$\sum_{a \in I_O} C_{ab}(x_a - x_b)e^{-\lambda(x_b)(x_a - x_b)} = w_b(x_b)$$

Assume to the contrary that (25) is not met. Then, λ blows up on the boundary. In fact, suppose that $\exists a \neq b : \lim_{x \rightarrow x_b} \frac{w_a(x)}{x-x_b} = \infty$ (note that this can be met even if $w_a(x_b) = 0$). Since $w_b(x_b)$ on the right-hand side of (26) is finite, which implies that (26) is met only if $\lim_{x \rightarrow x_b} \lambda(x) = \infty$. Finally, assume that I_O is empty, so that $w_a(x) = o(x - x_b) \forall a \in I \setminus \{b\}$, and hence $\lim_{x \rightarrow x_b} \frac{w_a(x)}{x-x_b} = 0$. Then, (26) is satisfied only if $\lim_{x \rightarrow x_b} \lambda(x) = -\infty$. \square

3.5.1. New prior Many priors that fulfil the conditions stipulated in Proposition 3.2 are readily constructed. However, as in the cases of global and *local* max-ent discussed earlier, it would be preferable to only have few basis function derivatives be non-zero on the boundary, namely two for first derivatives and three for second derivatives. With this in mind, we consider the following prior weight functions:

$$w_1(x) = 1, \quad w_a(x) = \left[\frac{(x - x_1)}{(x_a - x_1)} \right]^{(a-1)} \quad \forall a > 1 \quad (27)$$

In this case, since $w_a(x) = o(x - x_1) \forall a > 2$, $\lambda(x_1)$ is obtained by solving:

$$\lim_{x \rightarrow x_1} \left[\frac{w_2(x)}{(x - x_1)} \right] (x_2 - x_1) e^{-\lambda(x_2 - x_1)} = 1$$

with solution:

$$\lambda(x_1) = 0$$

From (23) it is readily inferred that only the first two basis functions will have non-zero first derivatives at $x = x_1$, whose value is given by the constraint equations. An analogous conclusion is drawn from (16) for the second derivatives. For this case, $\phi_3'(x_1) = 0$, and using (19) to compute $\phi_3''(x_1)$ yields

$$\lim_{x \rightarrow x_1} \frac{\phi_2(x)(x - x_1)}{\phi_3(x)} = \lim_{x \rightarrow x_1} \frac{w_2(x)e^{-\lambda x_2}(x - x_1)}{w_3(x)e^{-\lambda x_3}} = \frac{(x_3 - x_1)^2}{x_2 - x_1}$$

and therefore

$$\phi_3''(x_1) = \frac{2}{(x_3 - x_1)^2}.$$

If the grid is regular, the values of the other derivatives are:

$$\phi_1''(x_1) = \phi_3''(x_1) = \frac{2}{(x_3 - x_1)^2}, \quad \phi_2''(x_1) = \frac{-4}{(x_3 - x_1)^2}.$$

This expression is analogous to (20) for global max-ent, except for the fact that $x_3 - x_1$ appears instead of $x_2 - x_1$. If the grid is not regular, the derivatives are readily found using the constraint equations.

Remark

To render efficient computations in a domain that is discretized by many nodes, *priors* with compact support are desirable. So, only the neighbors of a sampling point x are required to be considered. In the presentation of the new priors, we assumed for the sake of clarity that $\phi_a(x_1) \neq 0$ for all a , and we bounded λ at just $x = x_1$. For any local *prior* (for example, Gaussian *prior* in [4]), we multiply the original prior weight functions ($w_a(x_1 + \epsilon) \neq 0$) by (27) so that locality is retained in the new *priors*, and λ and the derivatives of ϕ_a are bounded since (25) is met. A similar approach applies to bound λ and the derivatives of ϕ_a at $x = x_n$.

3.6. Numerical tests

In Figure 1, the first- and second-derivatives of global max-ent basis functions are plotted on a domain $\Omega = (0, 4)$, which is discretized by five nodes that are equi-spaced. As expected, $\phi_1'(0) = -1$, $\phi_2'(x_1) = 1$ and the other basis function derivatives are zero at $x = 0$. A similar result is observed at the end-point $x = 4$. The second derivatives are also in agreement with theory since the only non-zero second-derivatives at $x = 0$ are: $\phi_1''(0) = \phi_3''(0) = 2$, $\phi_2''(0) = -4$. Similarly, the predictions are verified at $x = 4$. When the nodal coordinate of x_2 is modified,

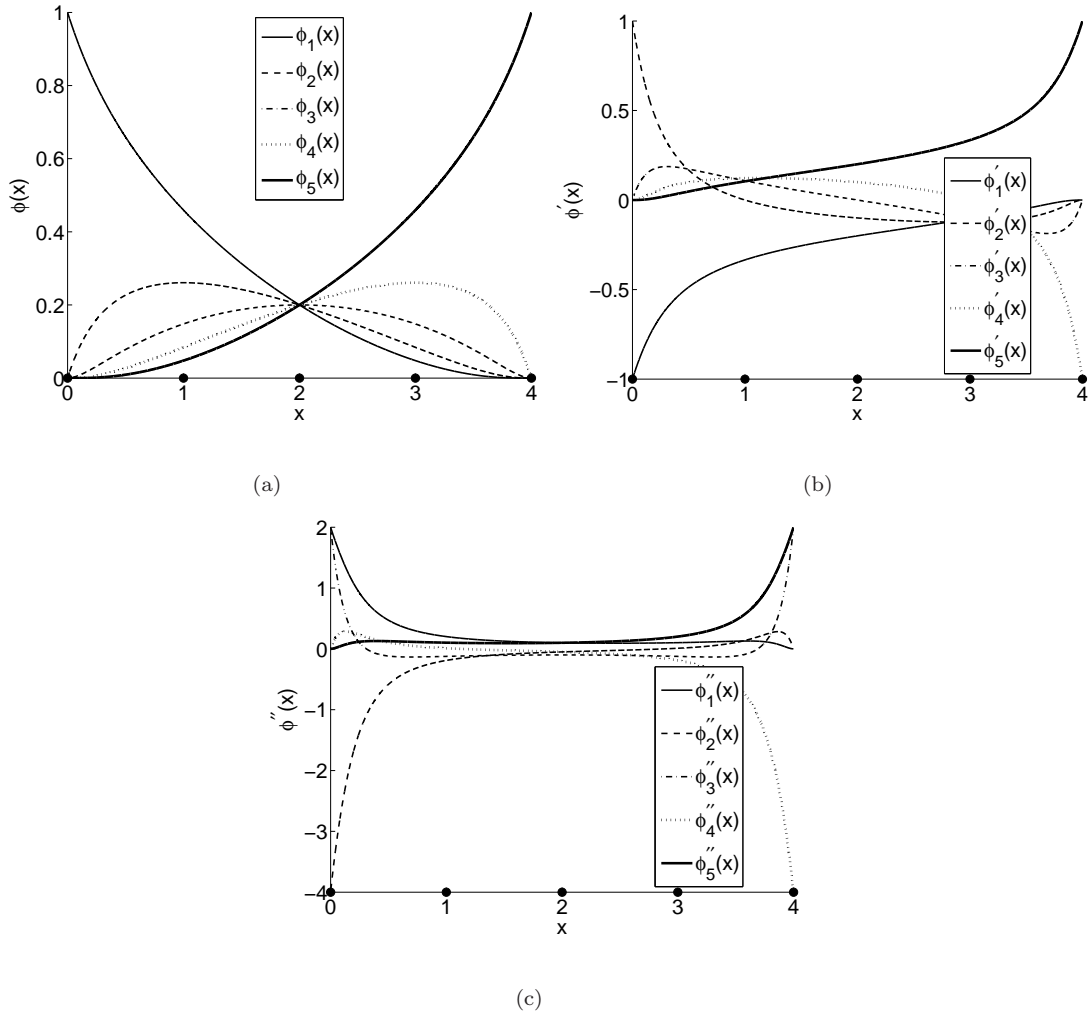


Figure 1. Derivatives of global max-ent basis functions on a regular grid. (a) $\phi_a(x)$; (b) $\phi'_a(x)$; and (c) $\phi''_a(x)$.

as in Figure 2, the second derivatives blow up at $x = 0$. This is more clearly observed on the logarithmic plot in Figure 3.

In Figure 4, the first- and second-derivatives for *local* max-ent basis functions ($\beta(x) = 1$) are plotted on the same regular grid. The values of the first derivative are not affected by the

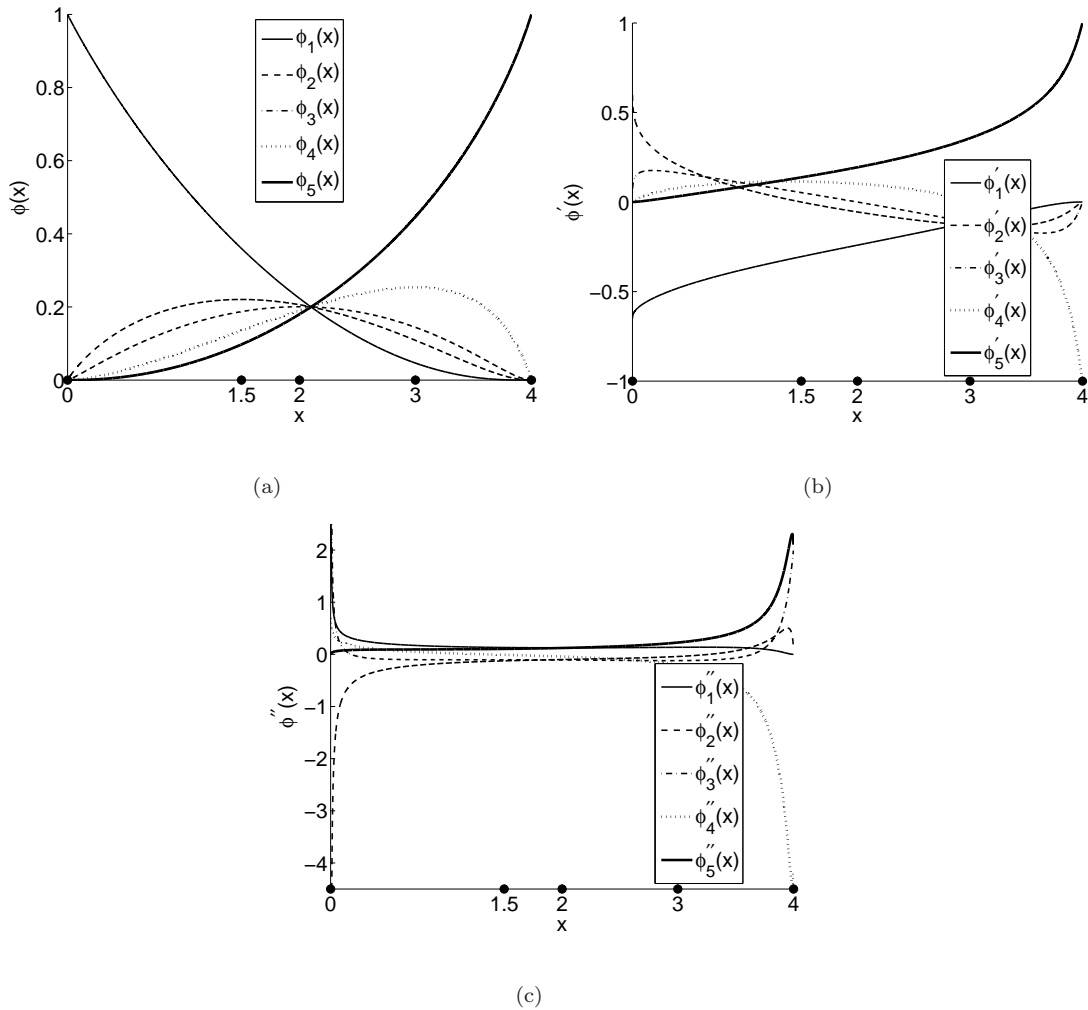
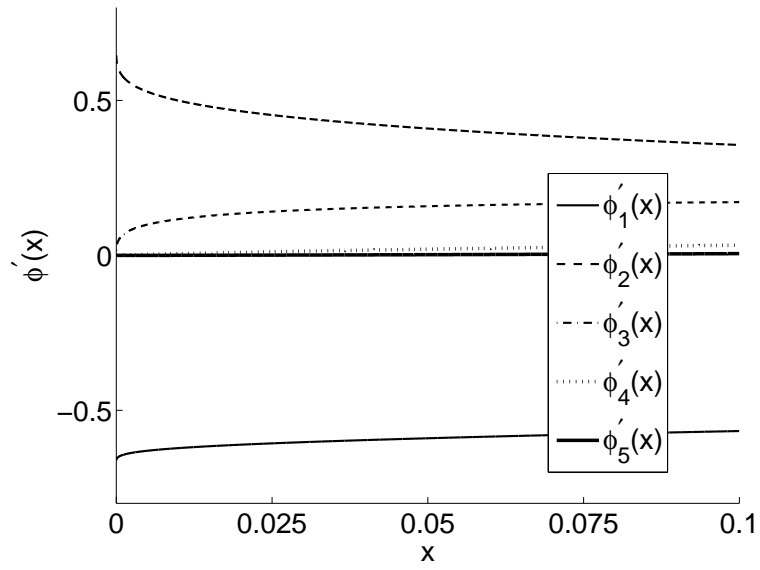


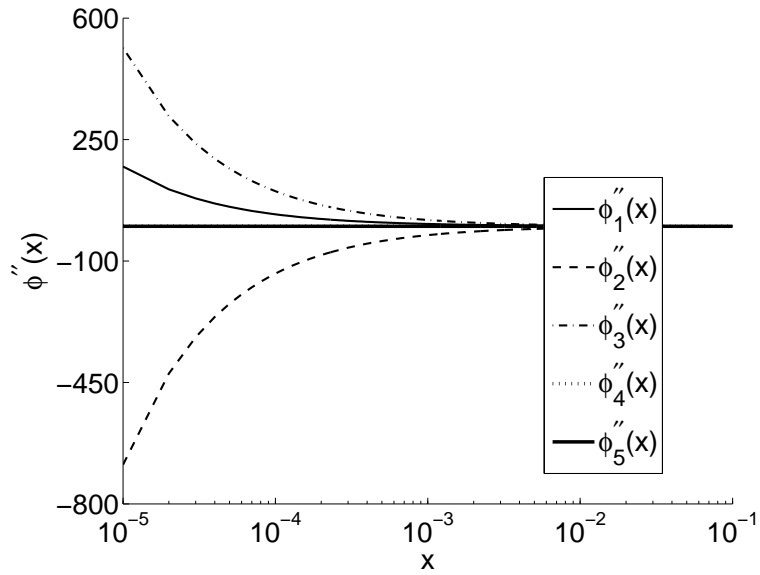
Figure 2. Derivatives of global max-ent basis functions on an irregular grid. (a) $\phi_a(x)$; (b) $\phi'_a(x)$; and (c) $\phi''_a(x)$.

introduction of this prior; however, now the second derivative of the basis functions have a different value, for example, $\phi''_1(0) = 2 \exp(-2) \sim 0.27$ from (22).

Finally in Figure 5, the effect of using the *new prior* given in (27) is depicted. Even on an irregular grid, the first derivatives of the basis functions have the same value as that realized



(a)



(b)

Figure 3. Plots of the derivatives of global max-ent basis functions near $x = 0$ on an irregular grid.

(a) $\phi'_a(x)$; and (b) $\phi''_a(x)$ on a logarithmic scale.

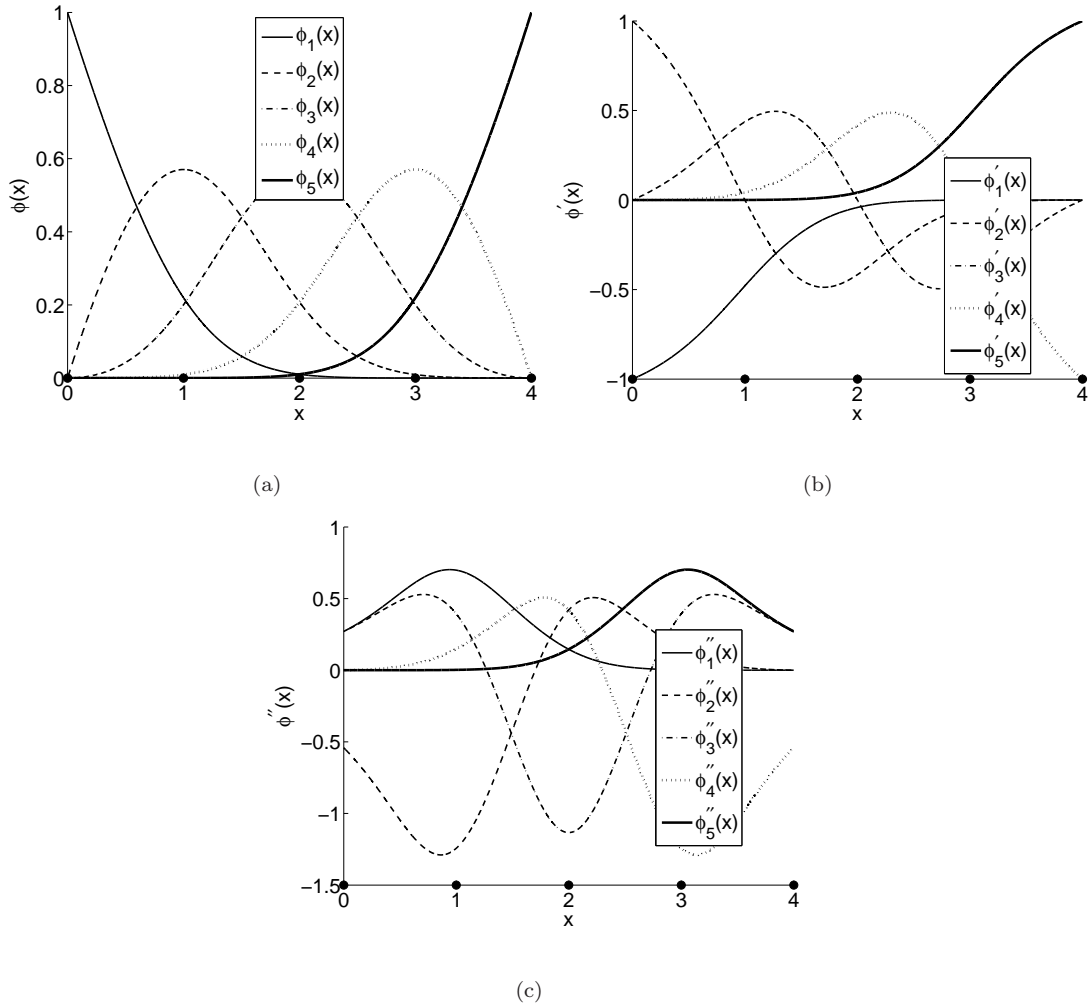


Figure 4. Derivatives of *local* max-ent basis functions on a regular grid. (a) $\phi_a(x)$; (b) $\phi'_a(x)$; and (c) $\phi''_a(x)$.

in global max-ent; however, the second derivatives of the basis functions are now bounded. We also note that $\phi''_3(0) = 1/2$, which is again in agreement with theory.

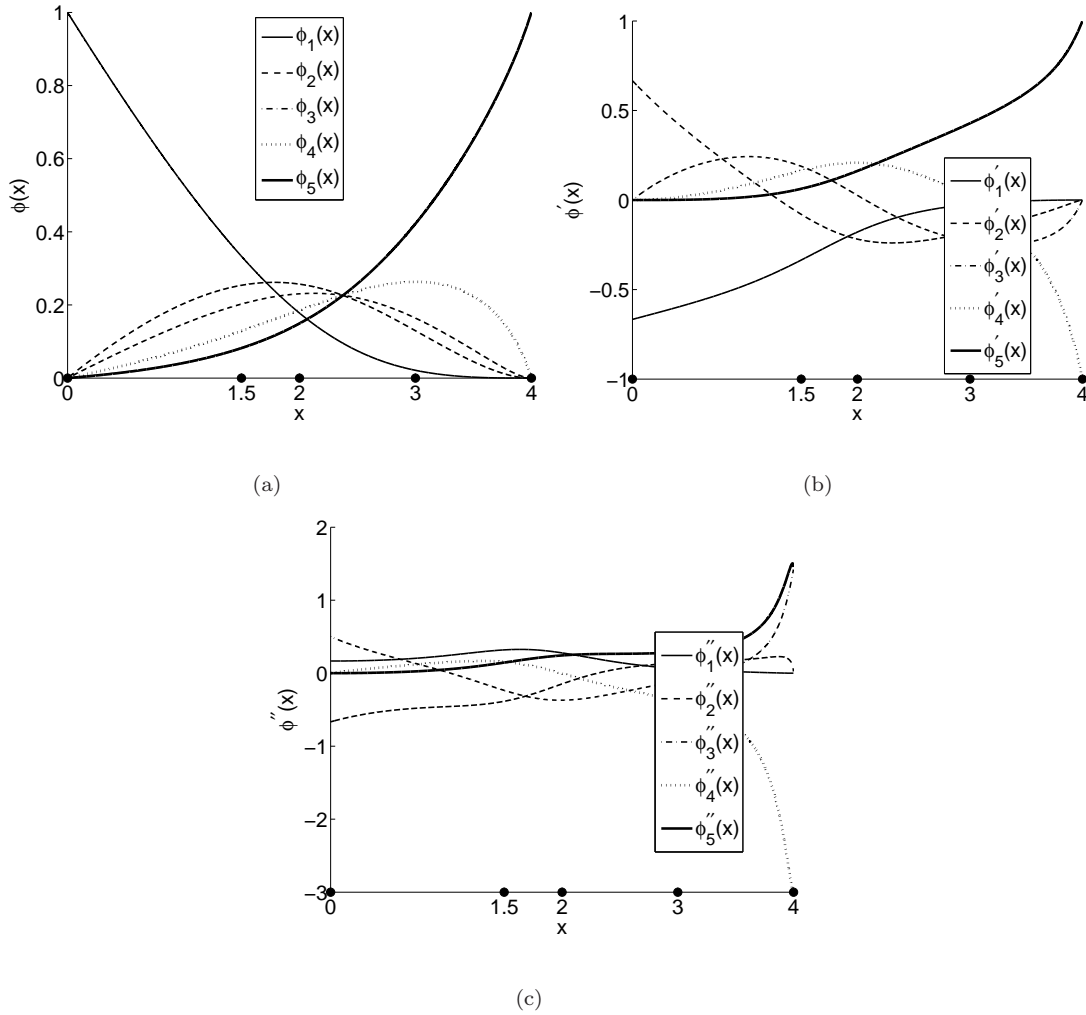


Figure 5. Derivatives of max-ent basis functions using the *prior* in (27). (a) $\phi_a(x)$; (b) $\phi'_a(x)$; and (c) $\phi''_a(x)$.

4. TWO-DIMENSIONAL ANALYSIS

Consider a two-dimensional convex domain $\Omega \subset \mathbb{R}^2$ that is discretized by a set of nodes with coordinates $\{\mathbf{x}_a\}_{a=1}^n$. We seek to evaluate the derivatives of the basis functions when $\mathbf{x} \in \partial\Omega$.

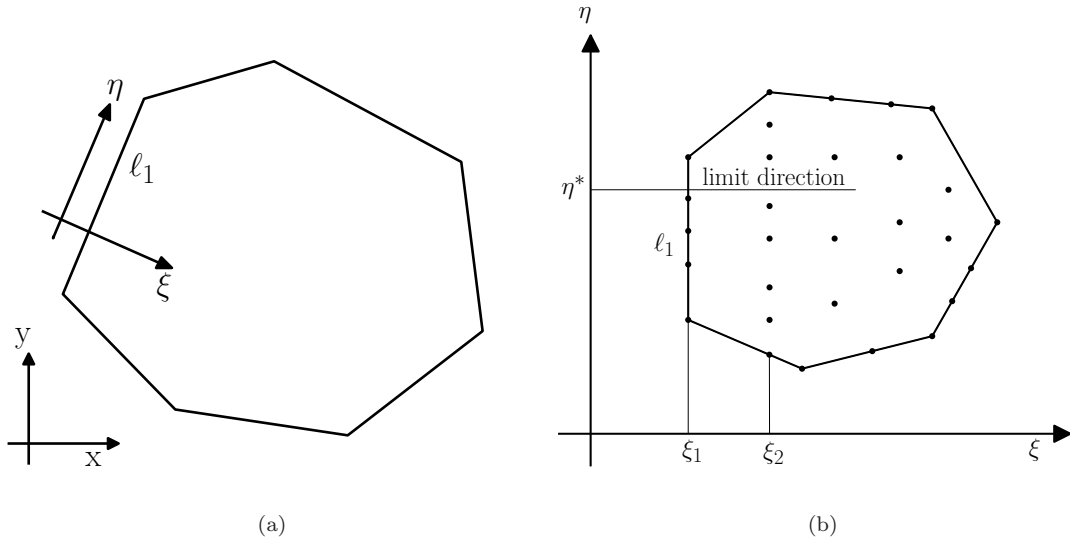


Figure 6. (a) Polygonal domain in the \mathbf{x} -coordinate system; and (b) Nodal discretization and the local ξ -coordinate system for the edge ℓ_1 .

4.1. First derivatives of local max-ent

The global max-ent approximant is a special case of the *local* max-ent (Gaussian *prior*) of Arroyo and Ortiz [4], and hence we directly consider the latter cognizant of the fact that in a Galerkin method a *prior* with compact-support is desirable.

A two-dimensional polygonal domain is shown in Figure 4.1, and we mark one of the boundary edges as ℓ_1 . Let $\xi \equiv (\xi, \eta)$ be a local coordinate system for the edge ℓ_1 . In Figure 4.1, a nodal discretization of the domain is shown in the local ξ -coordinate system. We seek to evaluate the derivatives of the nodal basis functions for points on the edge ℓ_1 . To this end, we proceed to determine the basis function derivatives $\nabla_{\xi} \phi_a$ in the ξ -coordinate system, and then through a linear (vector transformation), $\nabla \phi_a$ is obtained.

4.1.1. Tangential component of the gradient The evaluation of the tangential component $\frac{\partial \phi}{\partial \eta}$ is straightforward: it involves the variation of the basis functions on ℓ_1 (η -direction) and hence reduces to a one-dimensional problem on the edge ℓ_1 , since only nodes that lie on ℓ_1 have non-zero basis function values. Therefore, in this case, the basis functions and the tangential component of the gradient are obtained by considering the one-dimensional problem (η -coordinate of the nodes) along the edge ℓ_1 .

4.1.2. Normal component of the gradient As opposed to the tangential component, evaluating the normal component of the gradient requires additional effort, since the corresponding Lagrange multiplier ($\lambda(\xi)$) diverges, which can be readily shown via the two-dimensional counterpart of Proposition 3.1. With reference to Figure 6b, we evaluate the derivatives along ℓ_1 by extending the continuity of the derivatives from within the domain:

$$\frac{\partial \phi_a}{\partial \xi}(\xi_1, \eta) \equiv \phi_{a,\xi}(\xi_1, \eta) \equiv \lim_{\xi \rightarrow (\xi_1, \eta)} \phi_{a,\xi}(\xi)$$

Due to smoothness of the max-ent basis functions (excluding vertex locations), the result of the above limit has to be the same along any direction, and therefore we evaluate it along a convenient one. Let $\eta = \eta^*$ in Figure 6b be the normal direction for a given point on ℓ_1 . Then, consider $\lim_{\xi \rightarrow (\xi_1, \eta^*)} \frac{\phi_a(\xi)}{\phi_b(\xi)}$, where $\xi \rightarrow (\xi_1, \eta^*)$ along $\eta = \eta^*$. If both $\phi_a(\xi) \rightarrow 0$ and $\phi_b(\xi) \rightarrow 0$, we can apply l'Hôpital's rule:

$$\lim_{\substack{\xi \rightarrow (\xi_1, \eta^*) \\ \text{along } \eta = \eta^*}} \frac{\phi_a(\xi)}{\phi_b(\xi)} = \lim_{\xi \rightarrow \xi_1} \frac{\phi_{a,\xi}(\xi, \eta^*)}{\phi_{b,\xi}(\xi, \eta^*)}.$$

Since η is fixed, we follow the one-dimensional case to determine the non-zero derivatives on the boundary. Let ξ_1 be the ξ -coordinate of the nodes on ℓ_1 and ξ_2 be the ξ -coordinate of nodes on a line parallel to ℓ_1 (see Figure 6b). The nodes along ξ_1 and ξ_2 are indexed by the sets I_1 and I_2 , respectively. Note that $\phi_a = 0$ ($a \notin I_1$) for any point that lies on ℓ_1 . If $a \notin (I_1 \cup I_2)$

and $b \in I_2$ we can write

$$\lim_{\xi \rightarrow \xi_1} \frac{\phi_{a,\xi}(\xi, \eta^*)}{\phi_{b,\xi}(\xi, \eta^*)} = \lim_{\xi \rightarrow \xi_1} \frac{Z_a}{Z_b} = \lim_{\xi \rightarrow \xi_1} \frac{e^{-\beta\|\xi_a - \xi\|^2 - \lambda_1 \xi_a - \lambda_2 \eta_a}}{e^{-\beta\|\xi_b - \xi\|^2 - \lambda_1 \xi_b - \lambda_2 \eta_b}},$$

or

$$\lim_{\xi \rightarrow \xi_1} \frac{\phi_{a,\xi}(\xi, \eta^*)}{\phi_{b,\xi}(\xi, \eta^*)} = \lim_{\xi \rightarrow \xi_1} e^{-\beta(\|\xi_a - \xi\|^2 - \|\xi_b - \xi\|^2)} \times \lim_{\xi \rightarrow \xi_1} e^{-\lambda_1(\xi_a - \xi_b)} \times \lim_{\xi \rightarrow \xi_1} e^{-\lambda_2(\eta_a - \eta_b)},$$

where λ_1 and λ_2 are the Lagrange multipliers in the local ξ -coordinate system. Now, $\lambda_1 \rightarrow \infty$, λ_2 is bounded when $\xi \rightarrow \xi_1$, and since $\xi_a > \xi_b$, the right-hand side goes to zero and hence

$$\lim_{\xi \rightarrow \xi_1} \frac{\phi_{a,\xi}(\xi, \eta^*)}{\phi_{b,\xi}(\xi, \eta^*)} = 0.$$

Since η^* is arbitrary, we arrive at the result:

$$\phi_{a,\xi}(\xi_1, \eta) = 0 \quad \forall a \notin (I_1 \cup I_2). \tag{28}$$

Now, we consider the case when both $a, b \in I_2$. Then,

$$\lim_{\xi \rightarrow \xi_1} \frac{\phi_{a,\xi}(\xi, \eta^*)}{\phi_{b,\xi}(\xi, \eta^*)} = \lim_{\xi \rightarrow \xi_1} \frac{e^{-\beta\|\xi_a - \xi\|^2 - \lambda_1 \xi_a - \lambda_2 \eta_a}}{e^{-\beta\|\xi_b - \xi\|^2 - \lambda_1 \xi_b - \lambda_2 \eta_b}} = e^{-\lambda_2(\xi_1, \eta^*)(\eta_a - \eta_b) - \beta[(\eta_a - \eta^*)^2 - (\eta_b - \eta^*)^2]}, \tag{29}$$

where the Lagrange multiplier $\lambda_2(\xi_1, \eta^*)$ is linked to the one-dimensional problem, which is assessed in the following proposition:

Proposition 4.1. *The Lagrange multiplier $\lambda_2(\xi_1, \eta^*)$ from the two-dimensional problem corresponds to the Lagrange multiplier $\lambda(\eta^*)$ for the equivalent one-dimensional problem on the boundary.*

Proof. Consider the expression for the basis function $\phi_a(\xi)$, $a \in I_1$:

$$\phi_a(\xi) = \frac{e^{-\beta\|\xi_a - \xi\|^2 - \lambda_1 \xi_a - \lambda_2 \eta_a}}{\sum_{b=1}^n e^{-\beta\|\xi_b - \xi\|^2 - \lambda_1 \xi_b - \lambda_2 \eta_b}}$$

Since $\lambda_1 \rightarrow \infty$ when $\xi \rightarrow \xi_1$ the denominator can be approximated as

$$\sum_{b=1}^n e^{-\beta \|\xi_b - \xi\|^2 - \lambda_1 \xi_b - \lambda_2 \eta_b} \sim \sum_{b \in I_1} e^{-\beta \|\xi_b - \xi\|^2 - \lambda_1 \xi_b - \lambda_2 \eta_b}$$

and therefore $\phi_a(\xi)$ can be written as

$$\phi_a(\xi) = \frac{e^{-\beta \|\xi_a - \xi\|^2 - \lambda_2 \eta_a}}{\sum_{b \in I_1} e^{-\beta \|\xi_b - \xi\|^2 - \lambda_2 \eta_b}}.$$

Since $\xi_a = \xi_b = \xi_1$, $\xi \rightarrow \xi_1$ and $\eta = \eta^*$, the above equation simplifies to

$$\phi_a(\xi_1, \eta^*) = \frac{e^{-\beta(\eta_a - \eta^*)^2 - \lambda_2 \eta_a}}{\sum_{b \in I_1} e^{-\beta(\eta_b - \eta^*)^2 - \lambda_2 \eta_b}},$$

which is identical to the expression for the *local* max-ent basis functions at $\eta = \eta^*$ in one dimension. \square

Equation (29) reveals that in the two-dimensional case all the nodes that belong to the set I_2 (ξ -coordinate of ξ_2) have non-zero basis function derivatives on ℓ_1 and Proposition 4.1 allows us to compute the ratio between the derivatives. Hence, we now proceed as in the one-dimensional case. Consider the derivatives of the constraint equations in (2b) and (2c):

$$\sum_{a=1}^n \phi_{a,\xi}(\xi) = 0 \tag{30a}$$

$$\sum_{a=1}^n \phi_{a,\xi}(\xi) \xi_a = 1 \tag{30b}$$

which can be rewritten as

$$\begin{aligned} \sum_{a \in I_2} \phi_{a,\xi}(\xi_1, \eta) &= - \sum_{a \in I_1} \phi_{a,\xi}(\xi_1, \eta) \\ \xi_2 \sum_{a \in I_2} \phi_{a,\xi}(\xi_1, \eta) &= 1 - \xi_1 \sum_{a \in I_1} \phi_{a,\xi}(\xi_1, \eta) \end{aligned}$$

and on solving, we obtain

$$\sum_{a \in I_2} \phi_{a,\xi}(\xi_1, \eta) = \frac{1}{\xi_2 - \xi_1} \tag{31}$$

and hence the the derivatives for all the nodes that belong to I_2 is given by

$$\phi_{a,\xi}(\xi_1, \eta^*) = \frac{1}{(\xi_2 - \xi_1) \sum_{b \in I_2} e^{-\lambda_2(\xi_1, \eta^*)(\eta_b - \eta_a) - \beta[(\eta_b - \eta^*)^2 - (\eta_a - \eta^*)^2]}}, \quad a \in I_2.$$

Now, in order to complete the solution, we also require the derivatives of the basis functions for nodes $a \in I_1$. To this end, we begin with the expression for $\nabla \phi_a$ using *local* max-ent: $\nabla \phi_a^* = \phi_a^* \tilde{x}_a \cdot (\mathbf{H}^*)^{-1}$ from (6). Therefore, the explicit expression for the normal derivatives is given by

$$\phi_{a,\xi}(\boldsymbol{\xi}) = \phi_a(\boldsymbol{\xi}) \frac{\{ -(\xi - \xi_1) [\sum_{b=1}^n \phi_b(\boldsymbol{\xi}) \eta_b^2 - \eta^2] + (\eta - \eta_a) [\sum_{b=1}^n \phi_b(\boldsymbol{\xi}) \xi_b \eta_b - \xi \eta] \}}{[\sum_{b=1}^n \phi_b(\boldsymbol{\xi}) \eta_b^2 - \eta^2] [\sum_{b=1}^n \phi_b(\boldsymbol{\xi}) \xi_b^2 - \xi^2] - [\sum_{b=1}^n \phi_b(\boldsymbol{\xi}) \xi_b \eta_b - \xi \eta]^2}. \quad (32)$$

So, for nodes $a \in I_1$, we determine the limit of the above expression when $\xi \rightarrow \xi_1$. To this end, we divide all the terms by $(\xi - \xi_1)$. First, consider the term $\sum_{b=1}^n \phi_b(\boldsymbol{\xi}) \xi_b^2 - \xi^2$, which on rearranging yields

$$\begin{aligned} \sum_{b=1}^n \phi_b(\boldsymbol{\xi}) \xi_b^2 - \xi^2 &= \sum_{b \in I_1} \phi_b(\boldsymbol{\xi}) \xi_b^2 + \sum_{b \notin I_1} \phi_b(\boldsymbol{\xi}) \xi_b^2 - \xi^2 \\ &= \left(1 - \sum_{b \notin I_1} \phi_b(\boldsymbol{\xi}) \right) \xi_1^2 + \sum_{b \notin I_1} \phi_b(\boldsymbol{\xi}) \xi_b^2 - \xi^2 = \xi_1^2 - \xi^2 + \sum_{b \notin I_1} \phi_b(\boldsymbol{\xi}) (\xi_b^2 - \xi_1^2). \end{aligned}$$

If $b \notin I_1$, we can write

$$\lim_{\xi \rightarrow \xi_1} \frac{\phi_b(\boldsymbol{\xi}, \eta)}{\xi - \xi_1} = \lim_{\xi \rightarrow \xi_1} \frac{\phi_b(\boldsymbol{\xi}, \eta) - 0}{\xi - \xi_1} = \lim_{\xi \rightarrow \xi_1} \frac{\phi_b(\boldsymbol{\xi}, \eta) - \phi_b(\boldsymbol{\xi}_1, \eta)}{\xi - \xi_1} = \phi_{b,\xi}(\boldsymbol{\xi}_1, \eta) \quad (33)$$

and

$$\begin{aligned} \lim_{\xi \rightarrow \xi_1} \frac{\sum_{b=1}^n \phi_b(\boldsymbol{\xi}) \xi_b^2 - \xi^2}{\xi - \xi_1} &= \lim_{\xi \rightarrow \xi_1} \frac{\xi_1^2 - \xi^2 + \sum_{b \notin I_1} \phi_b(\boldsymbol{\xi}) (\xi_b^2 - \xi_1^2)}{\xi - \xi_1} \\ &= -2\xi_1 + \sum_{b \notin I_1} \phi_{b,\xi}(\boldsymbol{\xi}_1, \eta) (\xi_b^2 - \xi_1^2) = -2\xi_1 + (\xi_2^2 - \xi_1^2) \sum_{b \in I_2} \phi_{b,\xi}(\boldsymbol{\xi}_1, \eta) \\ &= \xi_2 - \xi_1 \end{aligned}$$

on using (31). The other expression that requires analysis is $\frac{\sum_{b=1}^n \phi_b(\boldsymbol{\xi}) \xi_b \eta_b - \xi \eta}{\xi - \xi_1}$. We again rearrange the numerator in this expression to obtain

$$\begin{aligned} \sum_{b=1}^n \phi_b(\boldsymbol{\xi}) \xi_b \eta_b - \xi \eta &= \xi_1 \sum_{b \in I_1} \phi_b(\boldsymbol{\xi}) \eta_b + \sum_{b \notin I_1} \phi_b(\boldsymbol{\xi}) \xi_b \eta_b - \xi \sum_{b=1}^n \phi_b(\boldsymbol{\xi}) \eta_b \\ &= \xi_1 \sum_{b \in I_1} \phi_b(\boldsymbol{\xi}) \eta_b + \sum_{b \notin I_1} \phi_b(\boldsymbol{\xi}) \xi_b \eta_b - \xi \left[\sum_{b \in I_1} \phi_b(\boldsymbol{\xi}) \eta_b + \sum_{b \notin I_1} \phi_b(\boldsymbol{\xi}) \eta_b \right] \\ &= (\xi_1 - \xi) \sum_{b \in I_1} \phi_b(\boldsymbol{\xi}) \eta_b + \sum_{b \notin I_1} \phi_b(\boldsymbol{\xi}) (\xi_b - \xi) \eta_b \end{aligned}$$

and since only ϕ_b ($b \in I_1$) are non-zero at $\xi = \xi_1$, then $\sum_{b \in I_1} \phi_b(\boldsymbol{\xi}) \eta_b = \eta$. Therefore,

$$\lim_{\xi \rightarrow \xi_1} \frac{\sum_{b=1}^n \phi_b(\boldsymbol{\xi}) \xi_b \eta_b - \xi \eta}{\xi - \xi_1} = -\eta + (\xi_2 - \xi_1) \sum_{b \in I_2} \phi_{b,\xi}(\xi_1, \eta) \eta_b$$

and since this limit exists, we have

$$\lim_{\xi \rightarrow \xi_1} \frac{[\sum_{b=1}^n \phi_b(\boldsymbol{\xi}) \xi_b \eta_b - \xi \eta]^2}{\xi - \xi_1} = 0$$

Accumulating all the results, the limit in (32) is:

$$\phi_{a,\xi}(\xi_1, \eta) = \lim_{\xi \rightarrow \xi_1} \phi_{a,\xi}(\boldsymbol{\xi}) = \frac{\phi_a(\xi_1, \eta)}{\xi_2 - \xi_1} \left\{ \frac{(\eta - \eta_a) [-\eta + (\xi_2 - \xi_1) \sum_{b \in I_2} \phi_{b,\xi}(\xi_1, \eta) \eta_b]}{\sum_{b=1}^n \phi_b(\xi_1, \eta) \eta_b^2 - \eta^2} - 1 \right\}$$

The above equation completes the evaluation of the derivatives along ℓ_1 , with the exception of the vertices of the polygon. For a point that approaches a vertex of the polygon, the denominator $\sum_{b=1}^n \phi_b(\xi_1, \eta) \eta_b^2 - \eta^2$ is zero. Thus, a further extension of continuity is required.

We note that as in (33), if η_1 and η_2 are the coordinates of the first two vertices in the η -direction, then

$$\lim_{\eta \rightarrow \eta_1} \frac{\sum_{b \in I_1} \phi_b(\xi_1, \eta) \eta_b^2 - \eta^2}{\eta - \eta_1} = \eta_2 - \eta_1$$

and if a is not one of the vertex-indices,

$$\lim_{\eta \rightarrow \eta_1} \frac{\phi_a(\xi_1, \eta)}{\eta - \eta_1} = \phi_{a,\eta}(\xi_1, \eta_1).$$

Hence, the expression of the derivatives at $\eta = \eta_1$ is given by

$$\phi_{1,\xi}(\xi_1, \eta_1) = \frac{1}{\xi_2 - \xi_1} \left\{ \frac{[-\eta_1 + (\xi_2 - \xi_1) \sum_{b \in \mathcal{I}_2} \phi_{b,\xi}(\xi_1, \eta_1) \eta_b]}{\eta_2 - \eta_1} - 1 \right\} \quad (34a)$$

$$\phi_{a,\xi}(\xi_1, \eta_1) = \frac{\phi_{a,\eta}(\xi_1, \eta_1)}{\xi_2 - \xi_1} \left\{ \frac{(\eta_1 - \eta_a) [-\eta_1 + (\xi_2 - \xi_1) \sum_{b \in \mathcal{I}_2} \phi_{b,\xi}(\xi_1, \eta_1) \eta_b]}{\eta_2 - \eta_1} \right\} \quad \forall a > 1 \quad (34b)$$

The *local* max-ent basis functions are $C^\infty(\Omega)$ in the interior of Ω [4], but are only C^0 at vertices of edges on the boundary of a two-dimensional convex domain. In Section 4.1.4, we present a numerical example that illustrates this behavior. The derivatives of the basis functions are discontinuous on the boundary of domains such as the one shown in Figure 6b.

4.1.3. Calculating the derivatives on the entire boundary The introduction of the local ξ -coordinate system eases the evaluation of the derivatives of the basis functions. The algorithm that follows summarizes the key steps that are needed in the computations:

- For each edge ℓ_α find all the neighbors of the nodes that contribute on ℓ_α .
- Transform the coordinates of all the neighbors from \mathbf{x} to ξ .
- Consider the equivalent one-dimensional problem on the boundary and evaluate the basis functions and their tangential derivatives. Store the value of the Lagrange multiplier $\lambda(\eta)$.
- Calculate the normal derivatives using the approach presented in Section 4.1.2.
- Transform $\nabla_\xi \phi_a$ to $\nabla \phi_a$ by a linear transformation, which involves a matrix-vector product. Note that in many applications this step is not necessary since only the normal derivatives are required.

4.1.4. Numerical tests In Figure 7a, a unit square is discretized by seven nodes and the partial derivatives $\frac{\partial \phi_a}{\partial x}$ are plotted along the edge $x = 0$ in Figure 7b. We observe that the

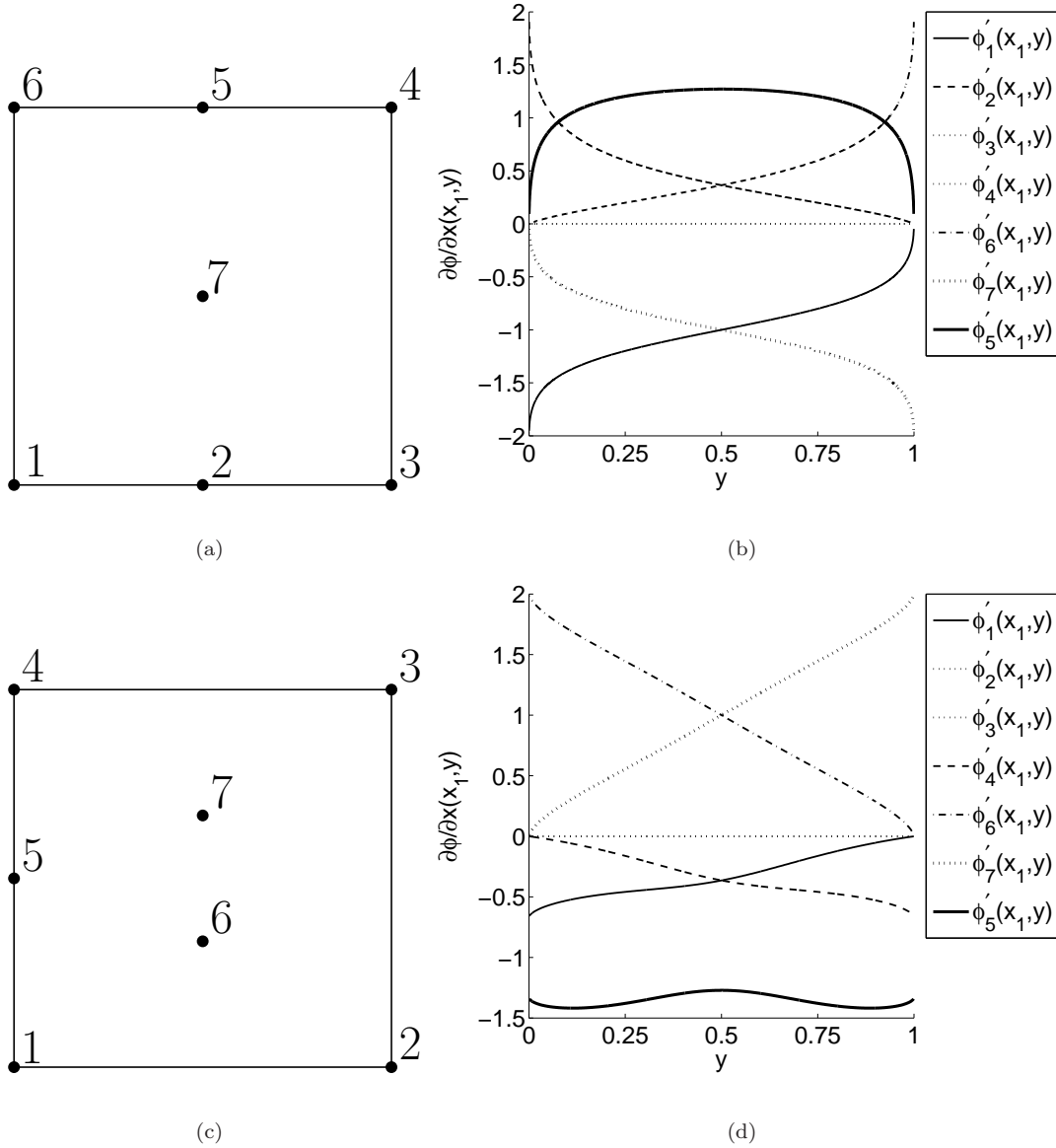


Figure 7. Partial derivative of basis functions in two dimensions. (a) Nodal discretization (grid 1); (b) $\frac{\partial \phi_a}{\partial x}$ along $x = 0$ for grid 1; (c) Nodal discretization (grid 2); and (d) $\frac{\partial \phi_a}{\partial x}$ along $x = 0$ for grid 2.

derivatives are smooth along the edge and at the vertices $(0, 0)$ and $(0, 1)$, the derivatives verify the continuity with the tangential derivatives of the adjacent edges. In Figure 7c, a different nodal discretization is shown and the plots of the derivative appear in Figure 7d. In this example, the derivatives are discontinuous at the vertices of the square. For instance at $(0, 0)$, we expect to obtain $\phi_{1,x} = -1$, $\phi_{a,x} = 0 \forall a > 2$ so that continuity with the tangential derivative on the edge $y = 0$ is met, with only $\phi_{1,x}$ and $\phi_{2,x}$ as non-zero. However, we find that $\phi_{1,x}$, $\phi_{5,x}$ and $\phi_{7,x}$ are non-zero, with their values computed from (34). This affirms that the max-ent basis functions are not smooth on the boundary of a domain.

4.2. Second derivatives of local max-ent

As in the one-dimensional case, the second derivatives are finite and non-zero only for a regular (structured) nodal discretization. An equation analogous to (18) is readily derived to establish that the second derivatives are finite and non-zero if and only if $\xi_3 - \xi_2 = \xi_2 - \xi_1$, where ξ_1 are the ξ -coordinate of the nodes on the boundary, ξ_2 are the ξ -coordinate of the nearest nodes to the boundary and ξ_3 the ξ -coordinate of the second-nearest nodes to the boundary.

4.3. Derivatives for other types of priors

The assessment in (28) holds for every *prior* that is non-zero on the boundary. Thus, the derivatives for the nodes with ξ -coordinate of ξ_2 can be evaluated using

$$\phi_{a,\xi}(\xi_1, \eta^*) = \frac{1}{(\xi_2 - \xi_1) \sum_{b \in I_2} \lim_{\xi \rightarrow \xi_1} \frac{\phi_a(\xi, \eta^*)}{\phi_b(\xi, \eta^*)}}$$

and then the derivatives for the nodes with ξ -coordinate of ξ_1 can be determined using an equation similar to (32), but with more terms in accordance with (6). The analysis is more complicated when the *priors* vanish on the boundary. In two dimensions, appropriate *priors*

can be defined that bound λ_1 on the boundary and therefore have finite first- and second-derivatives. However, as opposed to the one-dimensional case, the expressions for the *priors* are more involved.

Remark The extension to three-dimensions is straightforward. In this case, for each boundary-face of the domain, a normal out-of-plane component of the derivative of the basis functions exists along the direction ξ , and two tangential in-plane components are present along η and ζ . The computation of the latter is reduced to a two-dimensional problem, since only the nodes that lie on the $\eta\zeta$ -face have non-zero basis function values and therefore non-zero derivatives along the η - and ζ -directions. Then, as in the two-dimensional case, the derivatives of the nodes closest to the face are considered, and the derivatives on the $\eta\zeta$ -face are found by simplifying the limit in the three-dimensional counterpart of (32). Even though the expressions turn out to be lengthy, simplifications arise that are analogous to the two-dimensional case.

5. NUMERICAL EXAMPLES

The Galerkin solution of fourth-order ordinary and partial differential equations require the use of basis functions whose derivatives up to the second-order are square-integrable. In addition, the evaluation of the first derivatives of the basis functions on the boundary is required to impose boundary conditions. To verify the correctness and accuracy of the first- and second-derivatives of the max-ent basis functions on the boundary, we present Galerkin solutions to fourth-order problems using a quadratically complete enriched partition-of-unity max-ent approximation.

5.1. Euler-Bernoulli beam

Consider the governing equation for the deflection of an Euler-Bernoulli beam:

$$u''''(x) = q(x) \quad \text{in } \Omega = (a, b), \quad (35)$$

where $q(x)$ is the distributed load, and unit material parameters are assumed. Prior to including the boundary conditions, the weak statement of the above equation is: find $u \in \mathcal{U}$ such that

$$a(u, v) = \ell(v) \quad \forall v \in \mathcal{V}, \quad a(u, v) = \int_a^b u''v'' dx, \quad \ell(v) = \int_a^b q(x)v dx - u''v|_a^b + u'v'|_a^b. \quad (36)$$

In the above equation, the trial and test spaces are such that $\mathcal{U} = \mathcal{V} = H^2(\Omega)$, where $H^2(\Omega)$ is the Sobolev space with functions whose derivatives up to the second-order are square-integrable. When boundary conditions are specified, the trial and test spaces become subspaces of $H^2(\Omega)$. Note that the computation of the derivatives is required to evaluate the term $u''v'|_a^b$.

To solve fourth-order boundary-value problems using a Galerkin method, approximations that are quadratically complete are needed to ensure optimal rates of convergence. Prior work on constructing such approximations using non-negative max-ent basis functions appear in References [11, 13]. To verify our theoretical predictions with linearly precise max-ent, we adopt the framework of partition-of-unity [41–43] to construct an enriched approximation.

The quadratically-complete enriched max-ent approximation is:

$$u^h(x) = \sum_{a=1}^n \phi_a(x)u_a + \sum_{a=1}^n \psi(x)v_a = \sum_{a=1}^n \phi_a(x)u_a + \sum_{a=1}^n \phi_a(x)x^2v_a, \quad (37)$$

where $\psi_a(x) = \phi_a(x)x^2$ is the enriched basis function, and u_a and v_a are classical and enriched degrees of freedom, respectively. It should be noted that when such an enrichment is introduced the condition number of the stiffness matrix worsens [44, 45]. Our numerical tests confirm this prediction, but the increase in the condition number did not adversely affect accuracy nor its

rate of convergence on reasonably refined nodal discretizations. Improvements in the condition number via orthogonalization [46, 44] were tested, but these did not significantly improve the condition number to warrant its use in the present applications.

In order to mitigate errors due to numerical integration, we choose the following radial prior weight function:

$$w_a(r) = (1 - q^2)^4, \quad q \equiv q(r) = \frac{r}{\alpha h}, \quad r = |x - x_a|,$$

where $h = x_{a+1} - x_a$ is the nodal spacing and α is a parameter that determines the support size of the basis functions.

The performance of the enriched max-ent is compared to B -splines for the following model boundary-value problem:

$$u''''(x) = \sin(2\pi x) \quad \text{in } \Omega = (0, 1) \tag{38a}$$

$$u(0) = 0, \quad u''(0) = 0, \quad u(1) = 0, \quad u''(1) = 0. \tag{38b}$$

The exact solution of the above problem is: $u(x) = \sin(2\pi x)/(16\pi^4)$. Referring to (36), the linear form for this problem is: $\ell(v) = \int_0^1 \sin(2\pi x)v \, dx$. Any integration point in the domain for a k -th order B -spline approximation has $k+1$ neighbors (Figure 8a and Figure 8b). For a max-ent approximation with the radial *prior*, the number of neighbors at each integration points is 2α (Figure 8c and Figure 8d). In Figure 9, the B -spline and enriched max-ent solutions are presented. In Figure 9a, the $L^2(\Omega)$ norm of the error is plotted as a function of the degrees of freedom (DOFs); for the enriched max-ent, there are two degrees of freedom per node. We observe that the enriched max-ent solutions with $\alpha = 2$ and $\alpha = 3$ are comparable to the results obtained with quadratic and cubic B -splines, respectively. From Figure 9b, we observe that the enriched max-ent solution on a grid of four nodes is in good agreement with the exact solution.

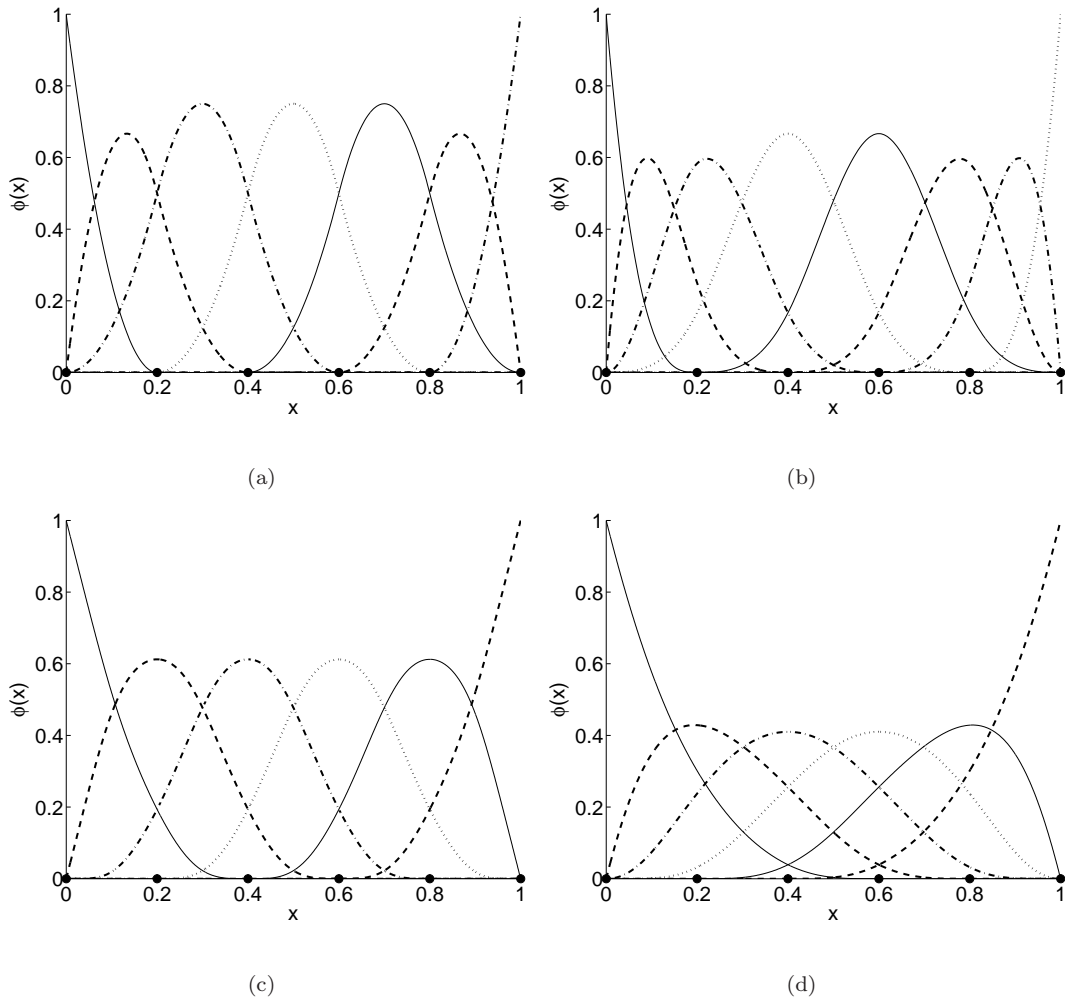


Figure 8. (a) Quadratic and (b) cubic B -spline basis functions on a regular grid. Maximum-entropy basis functions with a radial prior for (c) $\alpha = 2$ and (d) $\alpha = 3$ on a regular grid.

Having established the accuracy and convergence of the max-ent approximation, we now study the imposition of derivative boundary conditions by considering the following boundary-

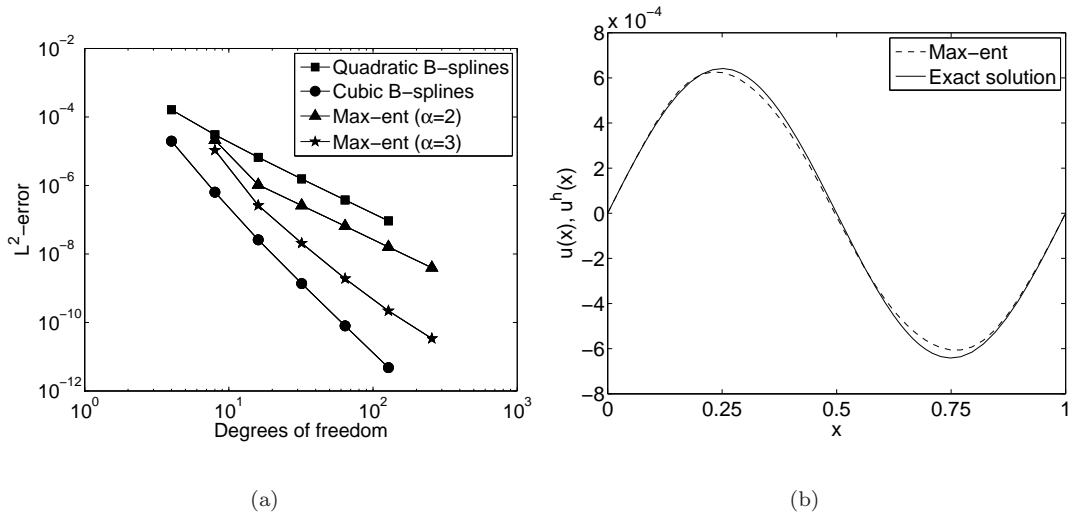


Figure 9. Comparisons of max-ent and B -splines for the model problem in (38). (a) $L^2(\Omega)$ norm of the error; and (b) Comparison between max-ent and the exact solution. Four nodes (8 DOFs) are used in the max-ent computations.

value problem:

$$u''''(x) = \sin(2\pi x) \quad \text{in } \Omega = (0, 1) \quad (39a)$$

$$u(0) = 0, \quad u'(0) = 0, \quad u''(1) = 2, \quad u'''(1) = 0, \quad (39b)$$

which is the model problem for a clamped cantilever beam (unit geometry and material parameters) with an applied moment at $x = 1$. The essential boundary condition $u^h(0) = 0$ is met by setting the coefficient $u_1 = 0$, as is done with finite elements. The enriched basis and its derivative vanish at $x = 0$: $\psi_a(0) = 0$, $\psi'_a(0) = 0$ for all a . From (12), only $\phi'_1(0)$ and $\phi'_2(0)$ are non-zero at $x = 0$. Hence, the essential boundary condition of zero-slope at $x = 0$ becomes $u_1\phi_1(0) + u_2\phi_2(0) = 0$, and therefore $u_1 = 0$ and $u_2 = 0$ must hold for both the essential boundary conditions to be satisfied.

Referring to (36), the linear form for this problem is: $\ell(v) = \int_0^1 \sin(2\pi x)v \, dx + 2v'(1)$, and

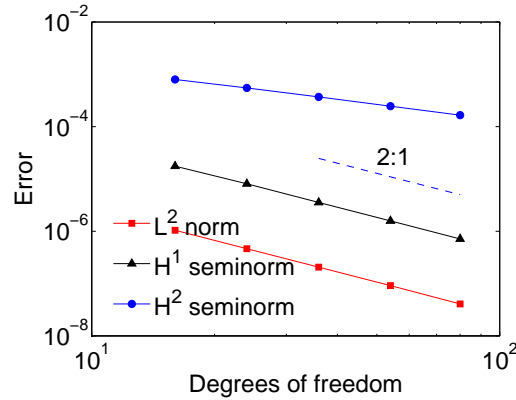


Figure 10. Rate of convergence for the model problem in (39).

hence the derivative of the basis functions (test functions) must be evaluated on the boundary $x = 1$. In order to demonstrate the accuracy of the imposition of the boundary conditions, the $L^2(\Omega)$ error norm, and $H^1(\Omega)$ and $H^2(\Omega)$ seminorms are plotted in Figure 10. A five-point Gauss quadrature rule is adopted; $\alpha = 2$ is used in the radial prior weight function. We obtain convergence rates of 2.0 in $L^2(\Omega)$ and $H^1(\Omega)$ seminorm, and a rate of 1.0 in $H^2(\Omega)$ seminorm. These rates are in agreement with theory [47], and similar rates of convergence are also reported in the recent work of Bompadre et al. [16, 48].

Lastly, we consider the free-vibration of a cantilever beam. Again, assuming unit material and geometry parameters, the eigenfrequencies are found by solving the following eigenproblem:

$$u''''(x) - \omega^2 u(x) = 0 \quad \text{in } \Omega = (0, 1) \quad (40a)$$

$$u(0) = 0, \quad u'(0) = 0, \quad u''(1) = 0, \quad u'''(1) = 0. \quad (40b)$$

where the values of k_n ($\omega_n = k_n^2$) are found by solving the nonlinear equation [49]:

$$\cos(k) \cosh(k) = -1.$$

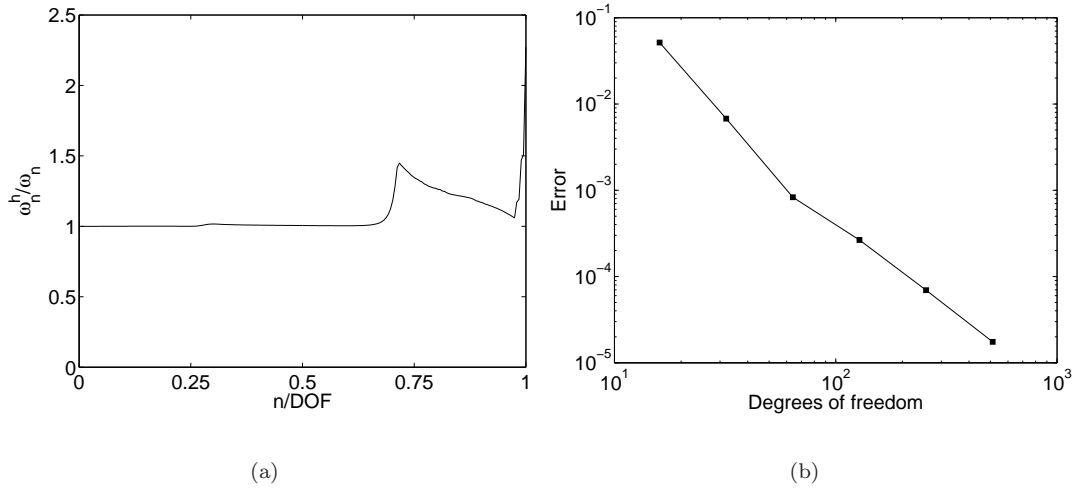


Figure 11. Eigenanalysis. (a) Ratio between the numerical (max-ent) and exact eigenfrequencies; and (b) Convergence in the error of the sum of the first 10 eigenfrequencies. The asymptotic rate of convergence is 2.0.

The weak form of the above eigenproblem is: find $u \in \mathcal{U}$, $\omega^2 \in \mathbb{R}_+$ such that

$$a(u, v) = \omega^2 b(u, v) \quad \forall v \in \mathcal{V}, \quad a(u, v) = \int_0^1 u'' v'' dx, \quad b(u, v) = \int_0^1 uv dx, \quad (41)$$

where \mathcal{U} and \mathcal{V} are the trial and test spaces, respectively. A 5-point Gauss quadrature rule, and $\alpha = 2$ in the radial *prior*, are used. In Figure 11a, the ratio of the numerical to the exact frequencies is plotted, and very good agreement is observed for the lower spectrum. The grid consists of 100 equi-spaced nodes (200 DOFs). In Figure 11b, convergence of the relative error in the sum of the lowest 10 eigenfrequencies is presented. The relative error is defined as:

$$\mathcal{E} = \frac{\sum_{n=1}^{10} (\omega_n^h - \omega_n)}{\sum_{n=1}^{10} \omega_n}$$

5.2. Plate bending

We consider plate bending (biharmonic operator) boundary-value problems in two dimensions. A quadratically-complete enriched max-ent approximation is used, with the following set of nodal basis functions:

$$\Phi_a = \{\phi_a, \phi_a x^2, \phi_a y^2, \phi_a xy\}. \quad (42)$$

The performance of the enriched max-ent method is studied for plate bending problems with a distributed load $q(\mathbf{x})$, with the governing equation (unit geometry and material parameters):

$$\nabla^4 u(\mathbf{x}) = q(\mathbf{x}) \quad \text{in } \Omega = (0, 1)^2, \quad (43)$$

which is supplemented with boundary conditions. If u and $\partial u/\partial n$ are prescribed, these become essential boundary conditions. Unlike the case of a clamped Euler-Bernoulli beam in one dimension, for a clamped plate in two dimensions with homogeneous essential boundary conditions, the nodal basis functions in (42) and their normal derivatives can not be made to vanish identically on the entire essential boundary (subset of $\partial\Omega$). To meet the essential boundary conditions, all coefficients must vanish that are associated with nodes that are proximal to the essential boundary, which would compromise the quadratic completeness of the approximation in Ω . For the clamped case, techniques such as Lagrange multipliers or Nitsche's method (see, for example, References [50, 51]) are widely used to impose essential boundary conditions.

In two dimensions, the imposition of natural boundary conditions is considered, which require the evaluation of the first-derivatives on the boundary. First, the model problem of a simply-supported plate with homogeneous essential and natural boundary conditions is

considered:

$$\begin{aligned}\nabla^4 u &= \sin(\omega x) \sin(\omega y) \quad \text{in } \Omega = (0, 1)^2 \\ u &= \nabla^2 u = 0 \quad \text{on } \partial\Omega.\end{aligned}$$

The weak form of the problem is:

$$a(u, v) = \ell(v) \quad \forall v \in \mathcal{V}, \quad a(u, v) = \int_{\Omega} \Delta u \Delta v \, d\Omega, \quad \ell(v) = \int_{\Omega} \sin(\omega x) \sin(\omega y) v \, d\Omega,$$

and the exact solution is given by

$$u(x, y) = \frac{1}{4\omega^4} \sin(\omega x) \sin(\omega y).$$

To impose the essential boundary condition ($u = 0$), all classical and enriched coefficients associated with nodes on the boundary are set to zero. We use *local* max-ent with $\beta = 1.25/h^2$, where h is the nodal-spacing. For the computations, a structured grid with uniform spacing in x - and y -directions is used, and a 7×7 tensor-product Gauss rule is used on the integration cells. The enriched max-ent solution shown in Figure 12a and the three-dimensional plot of the normalized error ($|u - u^h|/u_{\max}$) depicted in Figure 12b reveal the sound accuracy of the max-ent method. For these computations, a 15×15 grid (900 DOFs) with $\omega = 2\pi$ is used. The convergence of the max-ent solution for $\omega = \pi$ is presented in Figure 13, where the errors are plotted as a function of the number of nodes along each coordinate direction. The asymptotic rate of convergence in the $L^2(\Omega)$ error norm and the $H^1(\Omega)$ seminorm are 2.3, and the convergence rate in the $H^2(\Omega)$ seminorm is 1.1, which is consistent with theory [47].

As the next example, we consider prescribed (non-zero) moment conditions that are imposed on the boundary of the plate. The boundary-value problem is:

$$\nabla^4 u = 8 \quad \text{in } \Omega = (0, 1)^2 \tag{44a}$$

$$u = 0, \quad \nabla^2 u = 2(x^2 + y^2 - x - y) \quad \text{on } \partial\Omega. \tag{44b}$$

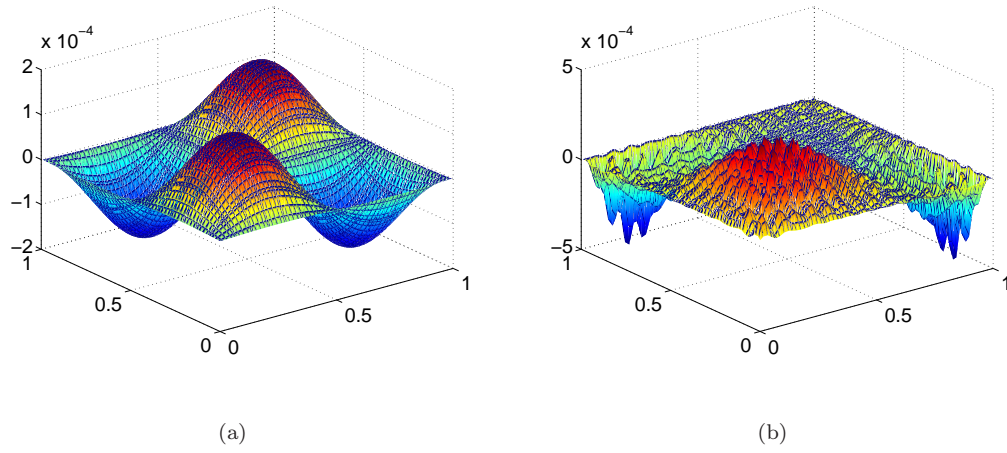


Figure 12. Simply-supported plate problem ($\omega = 2\pi$). (a) Enriched max-ent solution ; and (b) Normalized absolute error.

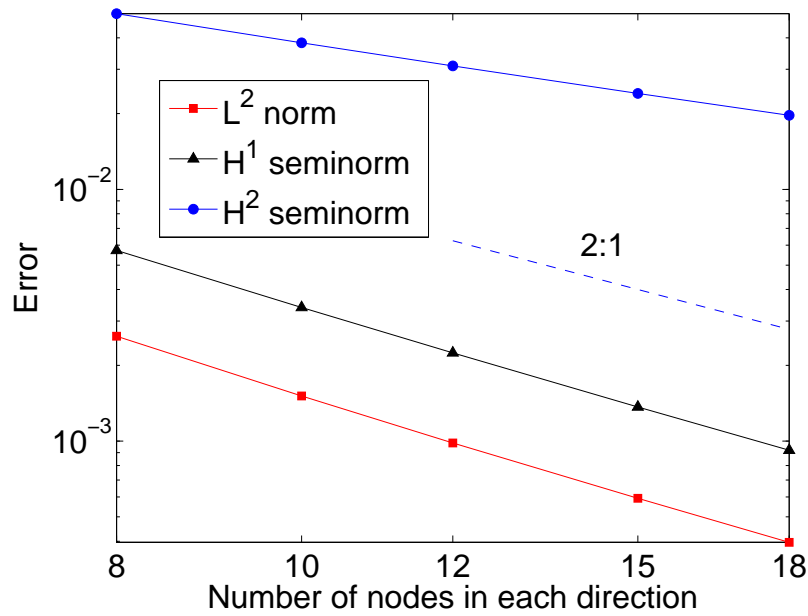


Figure 13. Rate of convergence for the simply-supported plate problem with homogeneous boundary conditions ($\omega = \pi$).

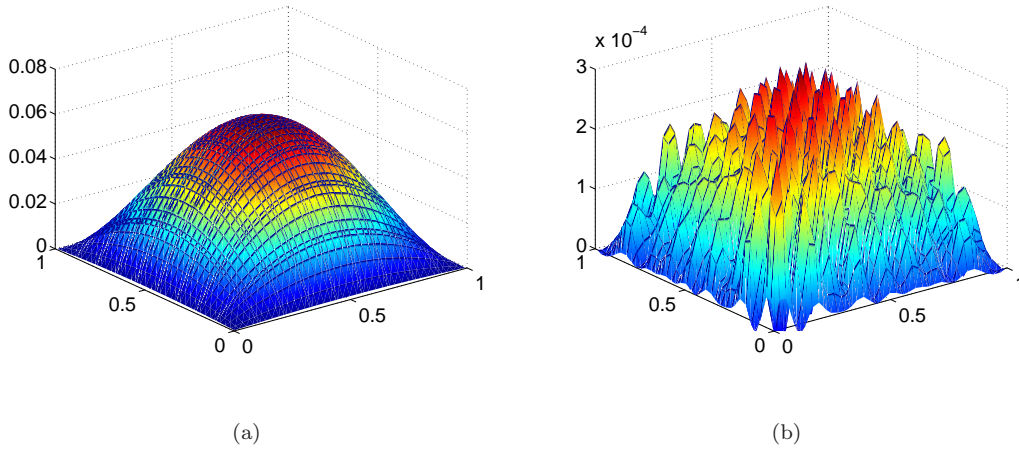


Figure 14. Accurate imposition of inhomogeneous natural boundary conditions for the simply-supported plate problem. (a) Enriched max-ent solution; and (b) Normalized absolute error.

with exact solution: $u(x, y) = xy(1 - x)(1 - y)$. The linear form $\ell(v)$ for this problem is:

$$\ell(v) = \int_{\Omega} 8v \, d\Omega + \int_{\partial\Omega} \frac{\partial v}{\partial n} D_{\Gamma} \, d\Gamma,$$

where D_{Γ} is the prescribed function $\nabla^2 u$ on the boundary, which is given in (44b). In the discrete system, the above expression for $\ell(v)$ yields the external (force) vector, which is computed by integrating the product of D_{Γ} and the normal derivative of the basis functions over the boundary of the domain.

For a 10×10 grid (400 DOFs), the enriched max-ent solution and the normalized error are plotted in Figure 14, and in Figure 15 the error norms are presented. These results reveal the good accuracy and convergence of the method. As in the previous example, asymptotic rates of convergence of 2.3 in $L^2(\Omega)$, 2.2 in $H^1(\Omega)$ seminorm, and 1.1 in $H^2(\Omega)$ seminorm are obtained, which are again consistent with theory [47].

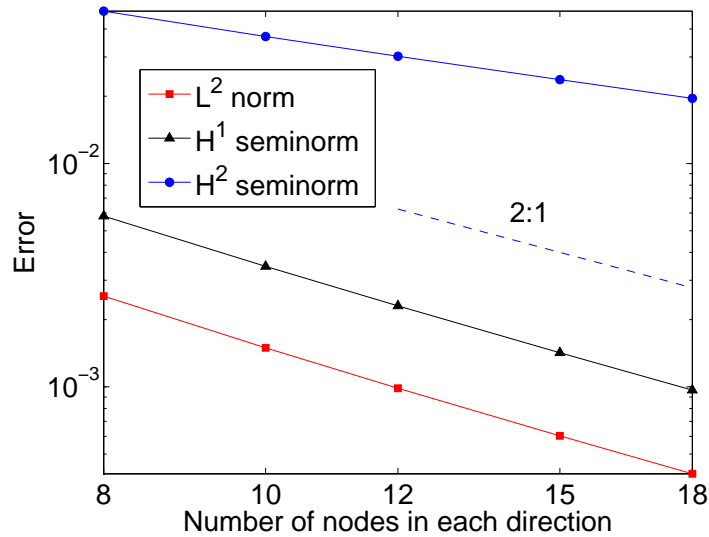


Figure 15. Rate of convergence for the simply-supported plate problem with inhomogeneous moment boundary conditions.

6. CONCLUDING REMARKS

In this paper, we have provided a solution to the open-problem of computing the derivatives of maximum-entropy basis functions on the boundary of a convex domain Ω . In the constrained optimization formulation, we considered the relative entropy as the objective functional with non-negative *prior* weight functions $w_a(\mathbf{x})$ assigned as an initial guess for each unknown basis function $\phi_a(\mathbf{x})$. On using the method of Lagrange multipliers, the expression for the derivatives of the basis functions that are obtained assume an indeterminate $0/0$ form for points $\mathbf{x} \in \partial\Omega$, which is a consequence of the divergence of the Lagrange multipliers. Since the Lagrange multipliers blow up on the boundary of the domain, the derivatives can not be directly computed for points $\mathbf{x} \in \partial\Omega$. Herein, we appealed to l'Hôpital's rule and used the constraint equations (linear reproducing conditions) to arrive at explicit expressions for the first- and

second-derivatives of the basis functions on the boundary. On regular and unstructured grids, we showed that the first-order derivatives of all basis functions were bounded on the boundary. In contrast, it was found that on an irregular grid with a certain nodal spacing, some of the second-derivatives of the basis functions were unbounded on the boundary. Necessary and sufficient conditions on the choice of the *priors* to obtain bounded Lagrange multipliers was established. To affirm the theoretical results, we adopted a quadratically-complete enriched maximum-entropy approximation to solve fourth-order problems. Simply-supported and clamped Euler-Bernoulli beam bending problems were considered and optimal convergence rates were obtained in the L^2 norm, and in the H^1 and H^2 seminorms. In two dimensions, simply-supported plate bending problems with zero and non-zero prescribed moments were considered, and we showed once again that the method was accurate and converged at the optimal rate. The expressions derived for the derivatives of the max-ent basis functions now also permit the evaluation of the strain and stress fields on the boundary.

ACKNOWLEDGEMENTS

The travel research fellowship awarded to Francesco Greco by the *Fondo Sociale Europeo* is gratefully acknowledged. The authors also thank Professor Luigi Filice for initiating and supporting the research visit of Francesco Greco to the University of California at Davis.

references

- [1] T. Belytschko, Y. Krongauz, D. Organ, M. Fleming, and P. Krysl. Meshless methods: An overview and recent developments. *Computer Methods in Applied Mechanics and*

- Engineering*, 139:3–47, 1996.
- [2] G. Fasshauer. *Meshfree Approximation Methods in MATLAB*. Interdisciplinary Mathematical Sciences – Vol. 6, World Scientific Publishers, Singapore, 2007.
- [3] N. Sukumar. Construction of polygonal interpolants: A maximum entropy approach. *International Journal for Numerical Methods in Engineering*, 61(12):2159–2181, 2004.
- [4] M. Arroyo and M. Ortiz. Local *maximum-entropy* approximation schemes: a seamless bridge between finite elements and meshfree methods. *International Journal for Numerical Methods in Engineering*, 65(13):2167–2202, 2006.
- [5] M. Arroyo and M. Ortiz. Local maximum-entropy approximation schemes. In M. Griebel and M. A. Schweitzer, editors, *Meshfree Methods for Partial Differential Equations III. Lecture Notes in Computational Science and Engineering 57*, pages 1–16, Springer, Berlin, 2007.
- [6] N. Sukumar. Maximum entropy approximation. *AIP Conference Proceedings*, 803(1):337–344, 2005.
- [7] C. E. Shannon. A mathematical theory of communication. *The Bell Systems Technical Journal*, 27:379–423, 1948.
- [8] R. T. Rockafellar. *Convex Analysis*. Princeton University Press, Princeton, NJ, 1970.
- [9] S. Boyd and L. Vandenberghe. *Convex Optimization*. Cambridge University Press, Cambridge, UK, 2004.

- [10] N. Sukumar and R. W. Wright. Overview and construction of meshfree basis functions: From moving least squares to entropy approximants. *International Journal for Numerical Methods in Engineering*, 70(2):181–205, 2007.
- [11] C. J. Cyron, M. Arroyo, and M. Ortiz. Smooth, second order, non-negative meshfree approximants selected by maximum entropy. *International Journal for Numerical Methods in Engineering*, 79(13):1605–2632, 2009.
- [12] D. González, E. Cueto, and M. Doblaré. A higher order method based on local maximum entropy approximation. *International Journal for Numerical Methods in Engineering*, 83(6):741–764, 2010.
- [13] A. Rosolen, D. Millán, and M. Arroyo. Second order convex *maximum entropy* approximants with applications to high order PDE. *International Journal for Numerical Methods in Engineering*, 2012. in press.
- [14] N. Sukumar and R. J-B Wets. Deriving the continuity of maximum-entropy basis functions via variational analysis. *SIAM Journal of Optimization*, 18(3):914–925, 2007.
- [15] A. Bompadre, B. Schmidt, and M. Ortiz. Convergence analysis of meshfree approximation schemes. *SIAM Journal of Numerical Analysis*, 50(3):1344–1366, 2012.
- [16] A. Bompadre, L. E. Perotti, C. J. Cyron, and M. Ortiz. Convergent meshfree approximation schemes of arbitrary order and smoothness. *Computer Methods in Applied Mechanics and Engineering*, 221-222:83–103, 2012.
- [17] K. Hormann and N. Sukumar. Maximum entropy coordinates for arbitrary polytopes. *Computer Graphics Forum*, 27(5):1513–1520, 2008. Proceedings of SGP 2008.

- [18] B. Li, F. Habbal, and M. Ortiz. Optimal transportation meshfree approximation schemes for fluid and plastic flows. *International Journal for Numerical Methods in Engineering*, 83(12):1541–1579, 2010.
- [19] A. Ortiz, M. A. Puso, and N. Sukumar. Maximum-entropy meshfree method for compressible and near-incompressible elasticity. *Computer Methods in Applied Mechanics and Engineering*, 199(25–28):1859–1871, 2010.
- [20] A. Ortiz, M. A. Puso, and N. Sukumar. Maximum-entropy meshfree method for incompressible media problems. *Finite Elements in Analysis and Design*, 47(6):572–585, 2011.
- [21] C. T. Wu and W. Hu. Meshfree-enriched simplex elements with strain smoothing for the finite element analysis of compressible and nearly incompressible solids. *Computer Methods in Applied Mechanics and Engineering*, 200(45–46):2991–3010, 2012.
- [22] W. Hu, C. T. Wu, and M. Koishi. A displacement-based nonlinear finite element formulation using meshfree-enriched triangular elements for two-dimensional large deformation analysis of elastomers. *Finite Elements in Analysis and Design*, 50(1):161–172, 2012.
- [23] A. Rosolen, D. Millán, and M. Arroyo. On the optimum support size in meshfree methods: A variational adaptivity approach with maximum-entropy approximants. *International Journal for Numerical Methods in Engineering*, 82(7):868–895, 2010.
- [24] D. Millán, A. Rosolen, and M. Arroyo. Thin shell analysis from scattered points

- with *maximum-entropy* approximants. *International Journal for Numerical Methods in Engineering*, 85(6):723–751, 2011.
- [25] D. Millán, A. Rosolen, and M. Arroyo. Nonlinear manifold learning for meshfree finite deformation thin shell analysis. *International Journal for Numerical Methods in Engineering*, 2012. DOI: 10.1002/nme.4403.
- [26] J. S. Hale and P. M. Baiz. A locking-free meshfree method for the simulation of shear-deformable plates based on a mixed variational formulation. *Computer Methods in Applied Mechanics and Engineering*, 241:311–322, 2012.
- [27] L. L. Yaw, N. Sukumar, and S. K. Kunnath. Meshfree co-rotational formulation for two-dimensional continua. *International Journal for Numerical Methods in Engineering*, 79(8):979–1003, 2009.
- [28] G. Quaranta, S. K. Kunnath, and N. Sukumar. Maximum-entropy meshfree method for nonlinear static analysis of planar reinforced concrete structures. *Engineering Structures*, 42:179–189, 2012.
- [29] C. J. Cyron, K. Nissen, V. Gravemeier, and W. A. Wall. Stable meshfree methods in fluid mechanics based on Green’s functions. *Computational Mechanics*, 46(2):287–300, 2010.
- [30] C. J. Cyron, K. Nissen, V. Gravemeier, and W. A. Wall. Information-flux maximum-entropy approximation schemes for convection-diffusion problems. *International Journal for Numerical Methods in Fluids*, 64(10–12):1180–1200, 2010.
- [31] K. Nissen, C. J. Cyron, V. Gravemeier, and W. A. Wall. Information-flux method: a meshfree maximum-entropy Petrov-Galerkin method including stabilised finite element

- methods. *Computer Methods in Applied Mechanics and Engineering*, 241–244:225–237, 2012.
- [32] A. Rosolen. *Developments in Maximum Entropy Approximants and Application to Phase Field Models*. Ph.D. thesis, Departament de Matemàtica Aplicada III, Universitat Politècnica de Catalunya, Barcelona, Spain, 2011.
- [33] F. Fraternali, C. D. Lorenz, and G. Marcelli. On the estimation of the curvatures and bending rigidity of membrane networks via a local maximum-entropy approach. *Journal of Computational Physics*, 231(2):528–540, 2012.
- [34] F. Fraternali and G. Marcelli. A multiscale approach to the elastic moduli of biomembrane networks. *Biomechanics and Modeling in Mechanobiology*, 2012. DOI: 10.1007/s10237-012-0376-9.
- [35] P. Suryanarayana, K. Bhattacharya, and M. Ortiz. A mesh-free convex approximation scheme for Kohn-Sham density functional theory. *Journal of Computational Physics*, 230(13):5226–5238, 2011.
- [36] E. T. Jaynes. Information theory and statistical mechanics. *Physical Review*, 106(4):620–630, 1957.
- [37] E. T. Jaynes. *Probability Theory: The Logic of Science*. Cambridge University Press, Cambridge, UK, 2003.
- [38] S. Kullback and R. A. Leibler. On information and sufficiency. *Annals of Mathematical Statistics*, 22(1):79–86, 1951.

- [39] J. E. Shore and R. W. Johnson. Axiomatic derivation of the principle of maximum entropy and the principle of minimum cross-entropy. *IEEE Transactions on Information Theory*, 26(1):26–36, 1980.
- [40] N. Sukumar. *Fortran 90 Library for Maximum-Entropy Basis Functions*. User's Reference Manual Version 1.4. Code available at , 2008.
- [41] J. M. Melenk and I. Babuška. The partition of unity finite element method: Basic theory and applications. *Computer Methods in Applied Mechanics and Engineering*, 139:289–314, 1996.
- [42] I. Babuška and J. M. Melenk. The partition of unity method. *International Journal for Numerical Methods in Engineering*, 40:727–758, 1997.
- [43] J. T. Oden, C. A. Duarte, and O. C. Zienkiewicz. A new cloud-based *hp* finite element method. *Computer Methods in Applied Mechanics and Engineering*, 153(1–2):117–126, 1998.
- [44] I. Babuška and U. Banerjee. Stable generalized finite element method (SGFEM). *Computer Methods in Applied Mechanics and Engineering*, 201:91–111, 2012.
- [45] M. A. Schweitzer. Generalizations of the finite element method. *Central European Journal of Mathematics*, 10(1):3–24, 2012.
- [46] E. Béchet, H. Minnebo, N. Moës, and B. Burgardt. Improved implementation and robustness study of the X-FEM for stress analysis around cracks. *International Journal for Numerical Methods in Engineering*, 64(8):1033–1056, 2005.

- [47] G. Strang and G. Fix. *An Analysis of the Finite Element Method*. Prentice-Hall, Englewood Cliffs, N.J., 1973.
- [48] A. Bompadre. Private communication. 2012.
- [49] W. Weaver, Jr., S. P. Timoshenko, and D. H. Young. *Vibration Problems in Engineering*. John Wiley & Sons, Inc., New York, fifth edition, 1990.
- [50] A. Embar, J. Dolbow, and I. Harari. Imposing Dirichlet boundary conditions with Nitsche's method and spline-based finite elements. *International Journal for Numerical Methods in Engineering*, 83(7):877–898, 2010.
- [51] T. Ruberg and F. Cirak. Subdivision-stabilised immersed b-spline finite elements for moving boundary flows. *Computer Methods in Applied Mechanics and Engineering*, 209:266–283, 2012.